

University of Szeged
Albert Szent-Györgyi Medical School
Doctoral School of Experimental and Preventive Medicine

Microglial activation is attenuated in cell culture by pharmacological modulation of calcium homeostasis

PhD Thesis



István Pesti

Supervisors: Prof. Dr. Eszter Farkas

Prof. Dr. Károly Gulya

Szeged, 2025

Publications related to the PhD thesis

- 1.** Pesti I, Légrádi Á, Farkas E.
Primary microglia cell cultures in translational research: Strengths and limitations.
Journal of Biotechnology, 2024 May 10;386:10-18. doi:
10.1016/j.jbiotec.2024.03.005. Epub 2024 Mar 20. PMID: 38519034.
- 2.** Pesti I, Barczánfalvi G, Dulka K, Kata D, Farkas E, Gulya K.
*Bafilomycin 1A Affects p62/SQSTM1 Autophagy Marker Protein Level and
Autophagosome Puncta Formation Oppositely under Various Inflammatory Conditions
in Cultured Rat Microglial Cells.*
International Journal of Molecular Sciences, 2024 Jul 29;25(15):8265. doi:
10.3390/ijms25158265. PMID: 39125836; PMCID: PMC11311604.
- 3.** Pesti I, Varga V, Qorri E, Frank R, Kata D, Vinga K, Szarvas PA, Menyhárt Á, Gulya K,
Bari F, Farkas E.
*Nimodipine reduces microglial activation in vitro as evidenced by morphological
phenotype, phagocytic activity and high-throughput RNA sequencing*
British Journal of Pharmacology, 2025, in press, doi: 10.1111/bph.70060 (BioRxiv:
doi: 10.1101/2024.11.11.623031)

Contents

Publications related to the PhD thesis	1
Abbreviations	4
1. Introduction	9
1.1 Microglia are central to neuroinflammation	9
1.1.1 Microglial activation is characterized by morphological and functional phenotypic changes	10
1.1.2 Autophagy modulates microglial activation	11
1.2 Alterations in calcium homeostasis are implicated in microglial activation	12
1.3 Nimodipine is a calcium channel blocker	13
1.4 Mechanisms and effects of DMT	15
1.5 Culture of microglia	17
1.6 Aims of the study	19
2. Materials and methods	20
2.1 Ethics declaration	20
2.2 Maintenance and treatment of primary microglia cell cultures	20
2.3 Immunohistochemistry	22
2.4 Western blot analysis	23
2.5 In vitro phagocytosis assay	24
2.6 Enzyme-linked immunosorbent assay (ELISA)	24
2.7 NEB mRNA-Library and next generation sequencing	24
2.8 LC-MS/MS analyses	25
2.9 Image analysis	26
2.10 Statistical analysis	27
3. Results	28
3.1 Nimodipine mitigates microglia activation	28
3.1.1 Nimodipine effect on microglial morphological phenotype	28

3.1.2 Nimodipine effect on microglial functional phenotype	29
3.1.3 Potential mechanisms of nimodipine effect on activated microglia	32
3.2 DMT modulates microglial activation.....	35
3.2.1 DMT effect on microglial morphological phenotype	36
3.2.2 DMT effect on microglial functional phenotype	36
3.2.3 Proteomic changes in microglia in response to DMT treatment	38
3.3 Suppression of autophagy in the presence of Baf.....	39
4. Discussion	40
4.1 Primary microglia cultures are suitable to study the pharmacological modulation of microglial activation	40
4.2 Microglial activation is characterized by changes in calcium homeostasis, which serve as a target to attenuate neuroinflammation.....	42
4.2.1 Benefits of nimodipine application for neuroinflammation	43
4.2.2 The therapeutic potential of DMT for neuroinflammation	45
4.3 The suppression of microglial autophagy is coincident with an increase in p62/SQSTM1 protein	47
5. Main observations and conclusions.....	49
6. Summary	50
7. Funding.....	53
8. Acknowledgements	53
9. References	54

Abbreviations

5-HT2A: 5-hydroxytryptamine (serotonin) 2A receptor

AADC: aromatic-L-amino acid decarboxylase

AD: Alzheimer's disease

AKT: protein kinase B

AMPA: α -amino-3-hydroxy-5-methyl-4-isoxazolepropionic acid

ANOVA: analysis of variance

APP: amyloid precursor protein

Baf: bafilomycin A1, ((3Z,5E,7R,8S,9S,11E,13E,15S,16R)-16-[(1S,2R,3S)-3-[(2R,4R,5S,6R)-2,4-dihydroxy-6-isopropyl-5-methyl-2-tetrahydropyranyl]-2-hydroxy-1-methylbutyl]-8-hydroxy-3,15-dimethoxy-5,7,9,11-tetramethyl-1-oxacyclohexadeca-3,5,11,13-tetraen-2-one)

BBB: blood-brain barrier

BDNF: brain-derived neurotrophic factor

BSA: bovine serum albumin

CALHM2: calcium homeostasis modulator family member 2

CaM: calmodulin

CaMKII: calcium/calmodulin-dependent protein kinase II

Cav: calcium voltage-gated channel

CCL: chemokine (C-C motif) ligand

Cd: cluster of differentiation

CFTCR: cystic fibrosis transmembrane conductance regulator

CNS: central nervous system

CPI-17: c-potentiated myosin phosphatase inhibitor of 17 kDa

CPM: counts per million

CREB: cAMP response element binding protein

CRAC: calcium release-activated calcium channel

CTSE: cathepsin E

CXCL10: C-X-C motif chemokine ligand 10

DAG: diacylglycerol

DAPI: 2-[4-(aminoiminomethyl) phenyl]-1H-indole- 6-carboximidamide hydrochloride

DEG: differently expressed gene

DFCP1: double FYVE containing protein 1

DIV: days in vitro

DMEM: Dulbecco's modified eagle's medium

DMT: N,N-dimethyltryptamine

DREAM: downstream regulatory element antagonist modulator

EDTA: ethylenediaminetetraacetic acid

ELISA: enzyme-linked immunosorbent assay

ER: endoplasmic reticulum

ERK1/2: extracellular signal-regulated protein kinases 1 and 2

FBS: fetal bovine serum

FDA: food and drug administration

FIZZ1: found in inflammatory zone 1

GAPDH: glyceraldehyde 3-phosphate dehydrogenase

HCD: higher-energy collision dissociation

HIF-1 α : hypoxia-inducible factor 1 α

HO-1: Heme oxygenase-1

Iba1: ionized calcium-binding adaptor molecule 1

IGF-1: insulin-like growth factor-1

iGluR: ionotropic glutamate receptor

IL: interleukin

INMT: indolethylamine N-Methyltransferase

iNOS: inducible nitric oxide synthase

IP3: inositol trisphosphate

IP3R: inositol trisphosphate receptor

IRE1: inositol-requiring enzyme 1

IRF: interferon regulatory factor

iROS: intracellular reactive oxygen species

LAMP2A: lysosome-associated membrane protein 2A.

LC3: microtubule-associated protein 1A/1B-light chain 3

LC-MS: liquid chromatography–mass spectrometry

LPS: bacterial lipopolysaccharide

MAM: mitochondria-associated ER membrane

MAO: monoamine oxidase

MHC: major histocompatibility complex

MLC: myosin light chain

MLCK: myosin light chain kinase

MLCP: myosin light chain phosphatase

MMP: matrix metalloproteinase

MMTS: S-methyl methanethiosulfonate

MS: mass spectrometry

mTOR/MTOR: mammalian target of rapamycin

MYPT1: myosin phosphatase target subunit 1

NCX: sodium-calcium exchanger

NF- κ B: nuclear transcription factor kappa B

NGS: next generation sequencing

NO: nitrogen oxide

NOS: nitrogen oxide synthase

NMDA: N-methyl-D-aspartate

NMDAR: N-methyl-D-aspartate receptor

OD: optical density

ORAI1: calcium release-activated calcium modulator 1

p62: ubiquitin-binding protein, 62 kDa (also known as sequestosome 1 (SQSTM1))

p70S6K: ribosomal protein S6 kinase β -1

PBS: phosphate-buffered saline

PCR: polymerase chain reaction

PD: Parkinson's disease

PDGF: platelet-derived growth factor

PGE₂: prostaglandin E2

PI3K: phosphatidylinositol 3-kinase

PI3KC3: phosphatidylinositol 3-kinase catalytic subunit type 3

PI3P: phosphatidylinositol 3-phosphate

PKC: protein kinase C

PLA2: phospholipase A2

PLC: phospholipase C

PLD3: phospholipase D family member 3

PPR: pattern recognition receptor

RhoA: ras homolog family member A

RNA-Seq: RNA-sequencing

ROS: reactive oxygen species

RT: room temperature

RT-qPCR: reverse transcription quantitative PCR

RyR: ryanodine receptor

S.D.: standard deviation

SDS: sodium dodecyl sulfate

SERCA: sarcoendoplasmic reticulum calcium ATPase

Sig-1R: sigma-1 receptor

subDIV: subcloned days in vitro

TBS: tris-buffered saline

TCEP: tris(2-carboxyethyl)phosphine

TEAB: tetraethylammonium bromide

TGF- β : transforming growth factor β

TI: transformation index

TLR: toll-like receptor

TMM: trimmed mean of M-values

TNF- α : tumor necrosis factor α

TRPM: transient receptor potential melastatin

TRPV: transient receptor potential vanilloid

UPR: unfolded protein response

V-ATPase: vacuolar ATPase

VEGF: vascular endothelial growth factor

VGCC: voltage-gated Ca^{2+} channels

VPS34: vacuolar protein sorting 34

Ym1/2: chitinase-like protein 3/2

1. Introduction

1.1 Microglia are central to neuroinflammation

Neuroinflammation is a complex inflammatory response in the central nervous system (CNS) potentially with adverse consequences. Parenchymal immunity in the brain is mediated by microglia, the brain's organ specific, tissue-resident macrophage population. The activation of microglia is a common pathological hallmark of chronic, prominent neurodegenerative disorders such as Alzheimer's disease and Parkinson's disease (Bartels et al., 2020; Leng and Edison, 2021), and acute brain injury including ischemic or hemorrhagic stroke and neurotrauma (Loane and Byrnes, 2010; Planas, 2024). In the healthy brain, microglia occupy a pivotal position in CNS development, maintenance of homeostasis, pruning of synapses, modulating neuronal plasticity and regulation of blood flow (Perry et al., 2013; Nimmerjahn et al., 2005; Kettenmann et al., 2011; Norris and Kipnis, 2019; Császár et al., 2022; Haruwaka et al., 2024). Under physiological conditions, microglia have a small cell body and highly ramified processes. This appearance corresponds to the quiescent state of microglia (Leyh et al., 2021). In response to exogenous danger signals like infection, or endogenous danger signals including ischemia, trauma, neurodegenerative diseases, or altered brain homeostasis, microglia transform from a resting to an activated state (Kreutzberg, 1996; Qin et al., 2023). Pathogen- and danger- associated molecular patterns are recognized by a variety of pattern recognition receptors (PPRs) on the microglial cell surface. Microglial cells express a variety of receptors on their membrane surface that aid in recognizing and engulfing molecules, particles, and cells (Fu et al., 2014; Sierra et al., 2013). Toll-like receptors (TLRs) represent one example of these PPRs that convey signals of danger, and intensely stimulate microglia during CNS damage or infection (Kigerle et al., 2014). This activation leads to rapid and profound changes in microglial morphology, function, and gene expression.

Activated microglia are identified by a change in morphology from a ramified state to an amoeboid state, which is characterized by enlarged cell bodies, shorter processes, and a more proliferative state. Exposure to typical activating agents like bacterial lipopolysaccharide (LPS) can readily induce these morphological modifications (Kettenmann et al., 2011; Hines et al., 2009). In addition to morphological changes, activated microglia exhibit distinct functional phenotypes that can be distinguished by focusing on migration, antigen presentation, phagocytosis, autophagy or metabolic program. As such, microglia are the specialized phagocytes of the CNS and play a critical role in sensing and engulfing extracellular material

such as cell debris, dying cells, cancer cells, and pathogens (Tremblay et al., 2011). Finally, the process of microglial activation has been shown to result in the secretion of numerous pro-inflammatory cytokines and chemokines, thereby inducing an increase in neuroinflammation (Wang et al., 2024).

1.1.1 Microglial activation is characterized by morphological and functional phenotypic changes

Microglial activation has both positive and negative consequences and can either promote neuroprotection or cause neuronal damage. The traditional classification distinguishes between classically activated microglia (referred to as M1 type) and alternatively activated microglia (known as M2 type), following the classification used for macrophages (Xiong et al., 2016). As illustrated in Figure 1.1, typical cell adhesion molecular patterns and the polarization-specific production profile of cytokines, chemokines, trophic factors and other mediators define the M1-M2 polarization state of microglia (Wendimu and Hooks, 2022). Importantly, the M1-M2 polarization is now recognized as a spectrum with intermediate, partially overlapping states (Jurga et al., 2020; Wendimu and Hooks, 2022). The inflammatory M1 subtype of microglia is typically triggered by Toll-like receptors and γ -interferon signaling. M1 microglia release pro-inflammatory cytokines like tumor necrosis factor- α (TNF- α), interleukin-6 (IL-6), IL-1, IL-1 β , and chemokines. When activated, microglia can become overactivated or dysregulated, these cells can release harmful substances like reactive oxygen species (ROS) and pro-inflammatory cytokines, which can lead to neuronal death. Conversely, M2 microglia exhibit anti-inflammatory properties and serve a neuroprotective function. In particular, M2 microglia enhance the production of arginase 1, release growth factors, and stimulate the secretion of anti-inflammatory cytokines, such as IL-10 and transforming growth factor β (TGF- β) (Colonna et al., 2017).

In summary, M1-M2 activated microglial polarization is a complex phenomenon in which the overlap of gene expression is not linear. Single-cell RNA sequencing shows that microglia simultaneously express M1 and M2 activation markers, and transcriptomic studies reveal a broader transcriptional profile (Qin et al., 2023).

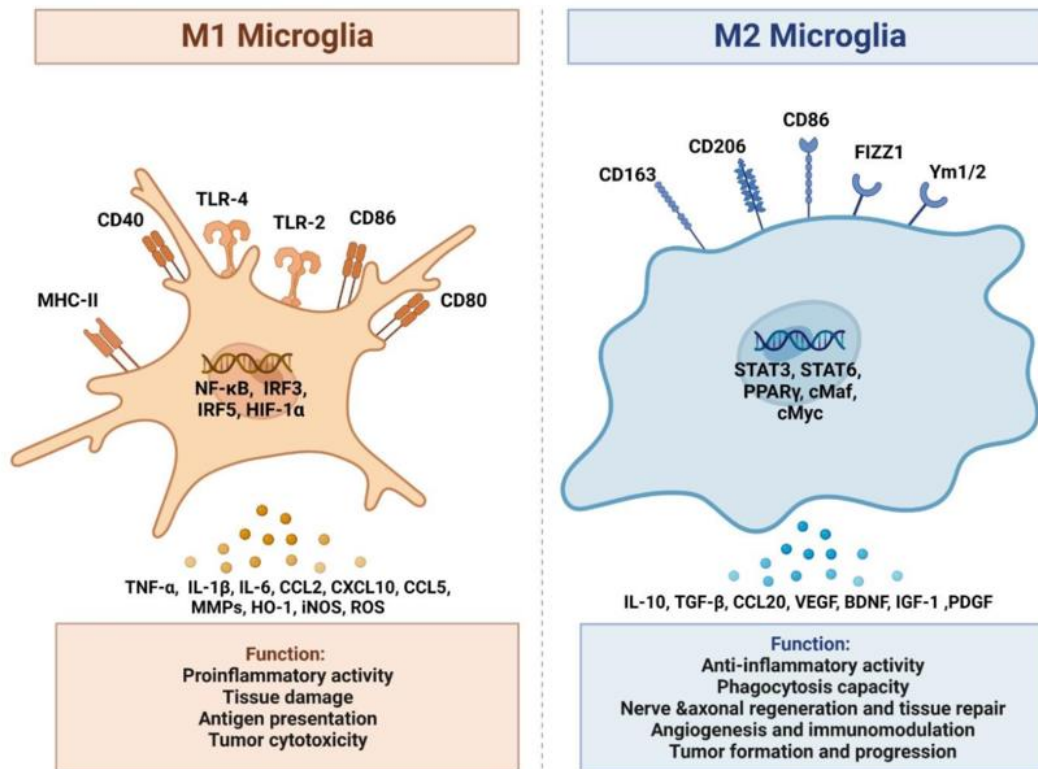


Figure 1.1 Morphological phenotypes of microglia correspond to their functional state. M1 microglia have been implicated in inflammatory processes, antigen presentation and the release of pro-inflammatory cytokines. M2 microglia have been shown to play a pivotal role in the reduction of inflammation through various mechanisms, including phagocytosis and the release of anti-inflammatory cytokines (Feng et al., 2024).

1.1.2 Autophagy modulates microglial activation

Autophagy influences cell metabolism and energy maintenance, contributing to cellular homeostasis. Under normal nutrient conditions, autophagy is low. However, under stress (e.g. ischemia, hypoxia, oxidative stress), autophagy can degrade and recycle cytoplasmic components. (Mugume et al., 2020).

Autophagy plays a crucial role in maintaining inflammation and immune balance to adapt to metabolic requirements. While it is known that autophagy can impact the polarization and function of microglia (Wang et al., 2023), the exact mechanism behind this process is still a topic of debate.

TLR4 has the potential to act as an upstream regulator of various signaling pathways that lead to autophagy-induced pro-inflammatory activation in microglia (Lee et al., 2018). Furthermore, lipopolysaccharide has the ability to activate the phosphatidylinositol 3-kinase (PI3K)/protein kinase B (AKT)/mammalian target of rapamycin (mTOR) pathway in microglia (Fig. 1.2), which in turn inhibits autophagic flow and enhances the inflammatory response (Ye et al., 2020). Conversely, activation of autophagy can inhibit the increase of LPS-induced pro-

inflammatory factors in microglia, thereby suppressing the inflammatory response (Han et al., 2013). The autophagy inhibitor bafilomycin A1 (Baf) has been shown to block microglia pro-inflammatory polarization (Qin et al., 2018).

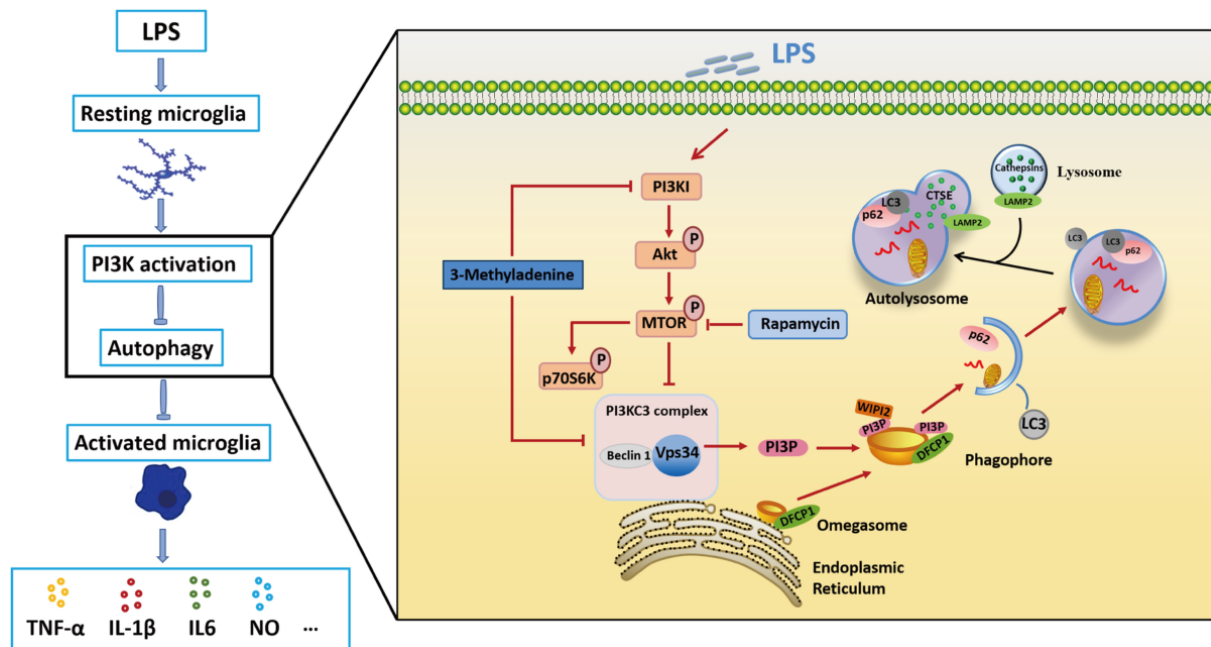


Figure 1.2 LPS exposure mediates the suppression of autophagy, which ultimately results in microglial activation. The activation of the mammalian target of rapamycin (MTOR) by lipopolysaccharide (LPS) has been demonstrated to exert an indirect inhibitory effect on the formation of autophagosomes. This, in turn, has been shown to result in an increase in the activation of microglial cells (Jin et al., 2018).

1.2 Alterations in calcium homeostasis are implicated in microglial activation

Intracellular Ca^{2+} concentration is tightly regulated because Ca^{2+} acts as a second messenger in various cellular signaling pathways. Intracellular Ca^{2+} also regulates the shift from a quiescent to an activated immune effector state of microglia. In resting cells, Ca^{2+} is present at a low concentration, whereas during activation the intracellular Ca^{2+} concentration increases rapidly (Eichhoff et al., 2011; Saddala et al., 2020). As such, exposure of cultured microglia to LPS revealed a sustained Ca^{2+} load of the cells (Hoffmann et al., 2003). Furthermore, variations in intracellular Ca^{2+} levels have been implicated in the regulation of microglial phagocytosis, proliferation, cytokine production, and release of reactive oxygen species (ROS) (Brawek & Garaschuk, 2013; Sharma & Ping, 2014).

Calcium influx across the plasma membrane in microglia is realized through various ion channels including voltage-gated Ca^{2+} channels (VGCCs), ligand-gated cation channels, transient receptor potential (TRP) cation channels, and Ca^{2+} release-activated Ca^{2+} channels (CRACs) (Fig. 1.3). Part of the Ca^{2+} influx must be mediated by L-type voltage-gated Ca^{2+} channels (VGCCs). In support of this notion, pharmacological antagonism of L-type voltage-gated Ca^{2+} channels (VGCCs) in

activated microglia reduced the intracellular Ca^{2+} load (Silei et al., 1999; Hegg et al., 2000), altered microglial superoxide production (Colton et al., 1994), and inhibited the production of the pro-inflammatory $\text{TNF-}\alpha$, $\text{IL-1}\beta$ and prostaglandin E_2 (PGE_2) (Li et al., 2009).

In addition to Ca^{2+} trafficking through cell surface channels, the endoplasmic reticulum (ER) also plays a role in regulating cytoplasmic calcium concentration during microglial activation (Neubrand and Sepúlveda, 2024). The ER serves as the major intracellular calcium store and is involved in Ca^{2+} release through ryanodine and IP_3 receptors and Ca^{2+} uptake through SERCA pumps. The involvement of ER-derived Ca^{2+} in microglial functional states has been shown by SERCA inhibition to reduce microglial phagocytosis (Morales-Ropero et al., 2021).

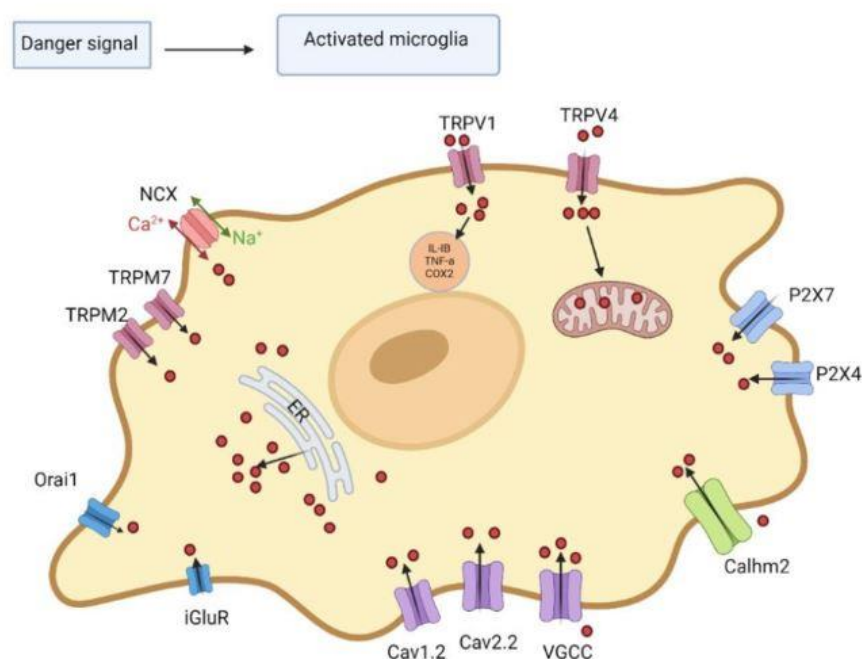


Figure 1.3 A synopsis of the regulation of calcium signaling in microglia highlights the pathways involved in calcium influx, release, and their contribution to cellular responses such as inflammation and gene expression. The influx of calcium into cells is facilitated by multiple channels, including transient receptor potential (TRP) channels and voltage-gated calcium channels (VGCCs). The release of calcium from the endoplasmic reticulum is orchestrated by inositol trisphosphate receptors (IP₃R) and ryanodine receptors (RyR) (Wang et al., 2024).

1.3 Nimodipine is a calcium channel blocker

Nimodipine is a dihydropyridine calcium antagonist, first synthesised in 1983 by Meyer and his colleagues. The molecular formula is $\text{C}_{21}\text{H}_{26}\text{N}_2\text{O}_7$ (Meyer et al., 1983). Nimodipine is a LVGCC blocker originally developed as a treatment for high blood pressure and now best known for its clinical application in the prevention of delayed ischemic deficit after

subarachnoid hemorrhage, for which the FDA approved its use in 1988. Nimodipine can be administered both orally and intravenously, but there are specific guidelines for each method.

The primary targets of nimodipine are cerebrovascular smooth muscle cells (Kazda and Towart, 1982), where vasorelaxation is achieved by inhibiting Ca^{2+} influx through LVGCCs. As a result, Ca^{2+} -dependent activation of smooth muscle cell contractile activity is reduced, cerebrovascular tone is decreased and cerebral blood flow is increased (Fig. 1.4). Because nimodipine is highly lipophilic and readily crosses the blood-brain barrier (Sin et al., 2018), and neurons also express LVGCCs (Bean, 1989), nimodipine has been tested as a neuroprotectant to prevent Ca^{2+} overload and associated neuronal injury (Espinosa-Parrilla et al., 2014). The therapeutic benefit of targeting neurons has remained inconclusive (Laskowitz and Kolls, 2010).

Recent studies raised the possibility that in addition to neurons, microglia also express LVGCCs, which may serve as a therapeutic target to attenuate neuroinflammation (Hopp, 2020). Microglia have been shown to express the Cav1.2 and Cav1.3 isoforms of the pore-forming α subunit of LVGCCs (Espinosa-Parrilla et al., 2015; Hopp, 2020), for which nimodipine affinity has been previously described (Huang et al., 2013; Xu and Lipscombe, 2001). We have recently demonstrated that nimodipine administered to the bath of live brain slice preparations challenged by mild oxygen-glucose deprivation shifts the morphological phenotype of activated microglia to resting state (Frank et al., 2024). However, we could not separate direct nimodipine effects on microglia from indirect actions (e.g. nimodipine altering neuronal excitation to which microglia respond), because LVGCCs are ubiquitously expressed in several cell types in the brain tissue, including neurons, astrocytes, and oligodendrocytes (Hopp, 2020).

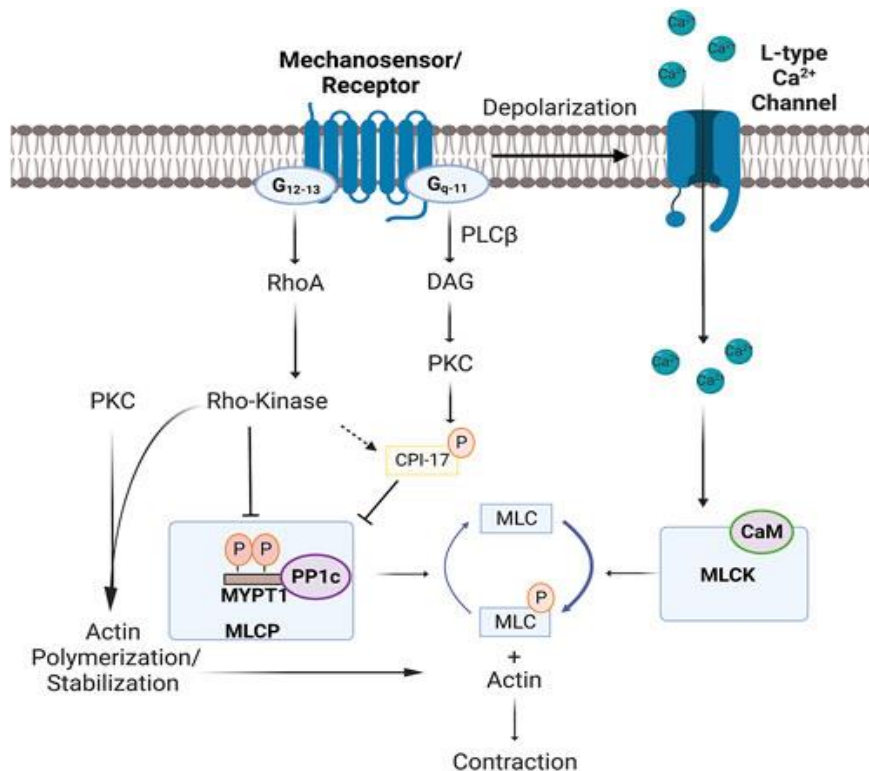


Figure 1.4 The mechanism of vascular smooth muscle contraction involves L-type voltage-gated Ca²⁺ channels. The activation of mechanosensory/receptive cells has been demonstrated to induce a process of depolarisation. This, in turn, has been shown to open L-type Ca²⁺ channels, resulting in an influx of Ca²⁺. The subsequent effect of this influx is to enhance myosin light chain (MLC) kinase (MLCK) and cross-bridge cycling through binding to CaM (Mironova et al., 2022).

1.4 Mechanisms and effects of DMT

N,N-dimethyltryptamine (DMT) is a naturally occurring indole alkaloid found in certain South American plants (e.g. *Psychotria viridis* and *Diplopterys cabrerana*). DMT has been demonstrated to have psychedelic effects and to cause hallucinations when consumed. DMT is a component of the traditional Ayahuasca brew used for centuries by indigenous tribes in the Amazon rainforest for spiritual and healing purposes (Carbonaro and Gatch, 2016). Furthermore, mammals synthesize DMT in small quantities, however, it is rapidly degraded in the body by monoamine oxidase (MAO) (Dean, 2018).

DMT has recently gained interest as a neuroprotectant in neurodegenerative diseases and acute ischemic brain injury (Penke et al., 2018). DMT was found to protect human primary iPSC-derived cortical neurons and microglia-like cells from hypoxia by decreasing HIF-1 expression and function (Szabo et al., 2016). DMT reduced infarct size in a rodent model of focal cerebral ischemia and showed anti-inflammatory effects by reducing pro-inflammatory cytokines (Nardai et al., 2020). DMT was also protective against apoptotic cell death in experimental global cerebral ischemia (Szabó et al., 2020). Based on the finding that DMT targets sigma-1 receptors (Sig-1Rs) in addition to serotonergic receptors, and binds to Sig-1Rs with high affinity (Fontanilla et al., 2009), ischemic neuroprotection by the compound has been attributed to its Sig-1R agonism (Szabo et al., 2021; Bouso et al., 2022).

Sig-1R is an intracellular receptor that is expressed in the brain, immune cells and various organs. It is situated within the ER membrane, specifically at the interface with mitochondria called the mitochondria-associated ER membrane (MAM). The primary function of Sig-1R is to regulate ATP synthesis by regulating Ca^{2+} levels (Sig-1R acts as a chaperone) (Weng et al., 2017). Sig-1R regulates Ca^{2+} transport between the MAM and mitochondria (Fig. 1.5), and also regulates intracellular Ca^{2+} levels by modulating the opening of cell surface NMDA receptors and VGCCs. Under physiological conditions, Sig-1R supports normal cellular homeostasis and energy production (Ren et al., 2022). In addition, Sig-1Rs have neuroprotective functions exerted by inducing cell survival under stress (Mori et al. 2013).

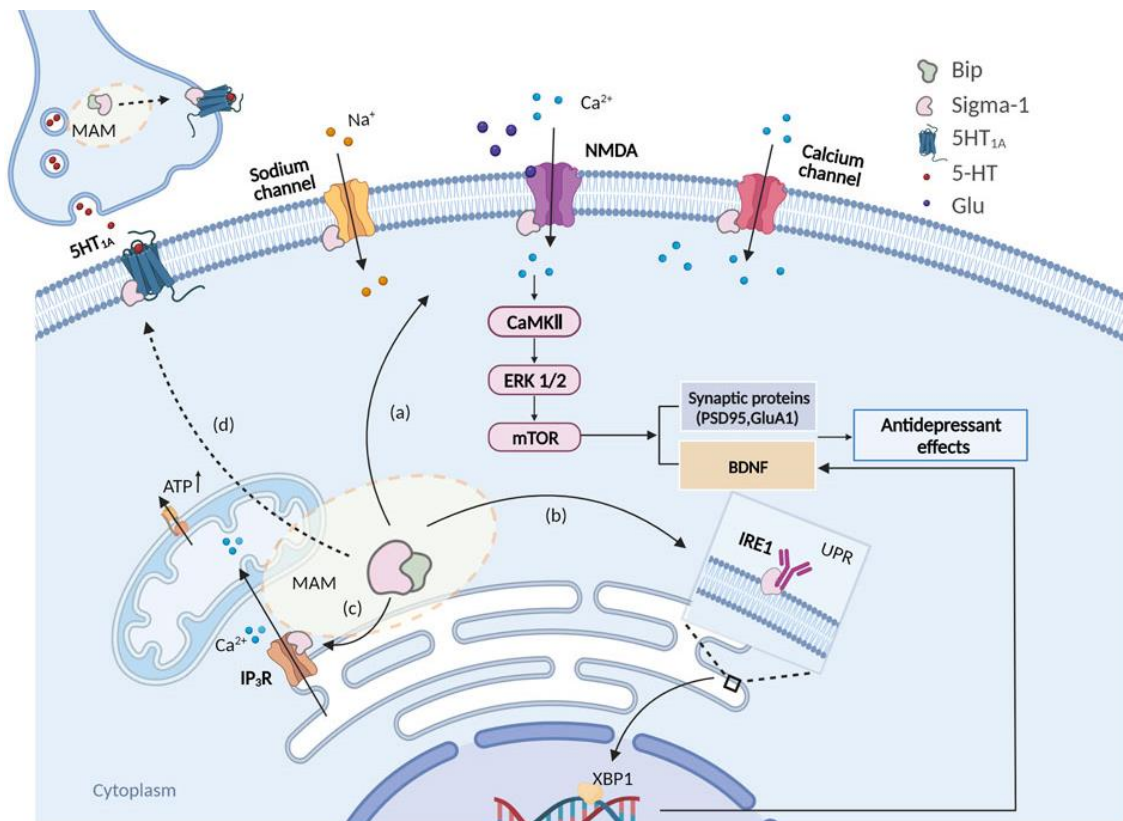


Figure 1.5. The intracellular signaling pathways of sigma-1 receptors contribute to Ca^{2+} trafficking between the endoplasmic reticulum (ER) and mitochondria and modulate cell surface ligand-gated cation channels. Sigma-1 receptors also stabilize IP₃R to maintain Ca^{2+} flow for ATP production and influence the ER stress response. Activated Sigma-1 receptors may also move to the plasma membrane, where they interact with NMDAR to activate CaMKII, impacting the mTOR pathways. (Ren et al., 2022).

The expression of sig-1Rs is ubiquitous in brain cells, encompassing neurons, astrocytes, oligodendrocytes, and microglia (Jia et al., 2018). In their study, Ooi and his colleagues demonstrated a decrease in Sig-1R and an increase in the M1 microglial marker CD86 in stressed rats. Treatment with SKF10047, a specific Sig-1R agonist, resulted in a reduction in

pro-inflammatory cytokines and a reversal of M1 microglial polarization. Furthermore, Sig-1R agonism in microglia cultures was found to suppress intracellular Ca^{2+} elevation in response to danger-associated molecular patterns. The Sig-1R activation in these experiments also restrained the microglial rearrangement of actin cytoskeleton, migration, and release of cytokines (Hall et al., 2009). These findings suggest that Sig-1R activation plays a role in reducing neuroinflammation by counteracting pro-inflammatory microglial activation (Ooi et al., 2021).

1.5 Culture of microglia

The use of simple preclinical model systems is warranted both by the tremendous complexity of microglial states in brain diseases and by the goal of developing new therapeutic tools. Primary microglial monocultures or co-cultures with neurons, astrocytes or oligodendrocytes are extensively used in studies of microglial pathophysiology. These tools allow reproducible, in-depth and high-throughput analysis of microglial states. Cell culture models are also essential for gaining valuable insights into microglial biology due to the controlled manipulation of experimental factors, the standardized experimental setting and the possibility of focused interpretation of results.

Primary microglial cultures are obtained from newborn rodent donor brains. The dissociated tissue provides a mixed cell suspension from which mixed cultures are initially grown as a confluent cell layer. Microglia are then mechanically separated to produce microglial monocultures with >95% purity. The most common way to activate microglia in culture is to add LPS to the culture medium. (Shi et al., 2010; Witting and Möller, 2011).

Microglia in culture can form diverse groups even without stimulation, indicated by their gene expression patterns (Cadiz et al., 2022). The activated microglial cultures are useful for testing drug candidates focused on neuroinflammation. This method allows estimates of drug effects on microglia without complicating factors from other brain cells (Sebastian-Valverde et al., 2021).

Microglia cultures enable the examination of morphological phenotypes. They can show whether microglia are inactivated (arborized) or activated (ameboid) by analyzing their shape (Szabo and Gulya, 2013). Functional aspects of microglia, such as migration, endocytosis, phagocytosis, autophagy, and metabolism, can be evaluated. Endocytosis and phagocytosis can be measured by adding specific fluorescent particles to the culture, which the microglia

internalize (Kata et al., 2016). Autophagy involves breaking down proteins and debris, which can be quantified by observing p62-positive particles (Ye et al., 2020).

Microglial states can be recognized through protein detection or gene expression profiling. Single-protein ELISA or multiplex ELISA are used to identify and quantify cytokines in culture media (Maguire et al., 2022). If the medium is serum-free, mass spectrometry can analyze the protein content comprehensively (Santiago et al., 2023). Western blotting measures selected proteins (Lam et al., 2017). Quantitative polymerase chain reaction quantifies specific nucleic acids, and single-cell RNA sequencing provides comprehensive gene expression profiles (Dumas et al., 2021).

Some of the strengths of rodent primary microglia cultures can also be considered limitations. These include a lack of genetic diversity due to inbreeding and sterile living conditions (Timmerman et al., 2018). However, the possibility to culture human microglia helps overcome this issue, despite the differences between rodent and human microglia (Smith and Dragunow, 2014). Microglia obtained from newborn rodents have not yet reached full maturity and are deficient in crucial interactions with other brain cells within their distinct environment. These interactions are imperative for microglia to effectively monitor neurons and maintain a quiescent state. The employment of mixed two-dimensional co-cultures, comprising cells such as astrocytes, facilitates a more comprehensive study of these interactions (Akhmetzyanova et al., 2024; Warden et al., 2023). Co-culturing microglia with neurons elucidates the impact of microglia on neuronal health, while co-culturing with oligodendrocytes investigates their function in myelin production (Roqué and Costa, 2017; Hamilton and Rome, 1994). The provision of appropriate cues is therefore paramount in ensuring the maintenance of a resting state in cultured microglia. The employment of advanced techniques is facilitating enhanced study practices for microglia in research.

Microglial cultures are easy to maintain, provide a consistent cell source, offer high cell numbers, are easily manipulated under controlled conditions, provide samples suitable for many assays, and generate reproducible data. As a result, these research tools will continue to be essential and complementary to *in vivo* investigations to explore therapeutic opportunities to combat the neurotoxic consequences of neuroinflammation associated with brain disorders.

1.6 Aims of the study

Our aim was to pharmacologically modulate microglia to suppress activation, and to elucidate the cellular mechanisms of pharmacological action:

1. We set out to analyze the effects of nimodipine on activated microglia at the level of morphological and functional phenotypes, as well as their transcriptomic profile. We hypothesized that nimodipine treatment suppresses microglial activation by acting on microglial Ca^{2+} homeostasis and associated changes in gene expression.
2. We sought to characterize the effects of DMT on microglial activation by morphological and functional profiling and by assessing changes in the microglial proteome. We anticipated an anti-inflammatory effect of DMT supported by an altered pattern of protein expression.
3. We aimed to identify the effect of the antibiotic bafilomycin on activated microglial autophagy. We assumed that bafilomycin mitigates microglial autophagy.

2. Materials and methods

2.1 Ethics declaration

All applicable international, national, and/or institutional guidelines for the care and use of animals were followed. Experimental procedures were carried out in strict compliance with the European Communities Council Directive (86/609/EEC) and followed Hungarian legislation requirements (XXVIII/1998 and 243/1998) and university guidelines regarding the care and use of laboratory animals. All experimental protocols were approved by the Institutional Animal Welfare Committee of the University of Szeged (I-74-II/2009/MÁB).

2.2 Maintenance and treatment of primary microglia cell cultures

Primary cortical microglia co-cultures (mixed with neurons, oligodendrocytes and astrocytes) were isolated from newborn rats, and microglial monocultures were derived from the co-cultures as previously described (Szabo and Gulya, 2013) and show in Figure 2.1. Briefly, cerebrocortical tissue from newborn Sprague-Dawley rat pups (P1) was rapidly dissected, minced, and dissociated in 0.25% trypsin for 10 min at 37°C. The trypsin was then neutralized with Dulbecco's modified Eagle's medium (DMEM) containing 1 g/L D-glucose, 110 mg/mL Na-pyruvate, 4 mM L-glutamine, 3.7 g/L NaHCO₃, 10,000 U/mL penicillin G, 10 mg/mL streptomycin sulphate, and 25 µg/mL amphotericin B and 15% heat-inactivated fetal bovine serum (FBS; Thermo Fisher Scientific, Carlsbad, CA, USA). After centrifugation at 1000g for 10 minutes at room temperature (RT), the pellet was resuspended, washed in 10 mL DMEM containing 10% FBS, and centrifuged again at 1000g and RT for 10 minutes. The final pellet was filtered through a sterile filter (100 µm pore size; Greiner Bio-One Hungary Kft., Mosonmagyaróvár, Hungary) to remove tissue fragments that had resisted dissociation. The cells were resuspended in 2 mL of the same solution and then seeded on poly-L-lysine-coated culture flasks (75 cm²; 10⁷ cells/flask) or poly-L-lysine-coated coverslips (15×15 mm; 2×10⁵ cells/coverslip) for immunocytochemistry or in poly-L-lysine-coated Petri dishes (60 mm × 15 mm; 10⁶ cells/Petri dish) for Western blot analysis and cultured at 37°C in a humidified air atmosphere supplemented with 5% CO₂. The medium was changed the next day and every 3 days thereafter. After 7 days of culture, microglial cells in primary co-cultures (DIV7) were shaken on a platform shaker (120 rpm for 20 min) at 37°C, the supernatant was collected by centrifugation (3000g for 8 min at RT), resuspended in 2 mL DMEM/10% FBS, and seeded in the same medium either on poly-L-lysine-coated coverslips (15×15 mm; 2×10⁵ cells/coverslip)

for immunocytochemistry or in poly-L-lysine-coated Petri dishes (60 mm × 15 mm; 10⁶ cells/dish) for Western blot analysis. The number of cells collected was determined in a Bürker chamber after trypan blue staining. DMEM/10% FBS was replaced the next day and then on the third and sixth day of subcloning (subDIV6).

Primary DIV6 co-cultures and microglia subDIV6 monocultures were challenged with lipopolysaccharide (LPS, dissolved in DMEM, 20 ng/mL in final concentration; Sigma, St. Louis, MO, USA) (Kata et al., 2016) and treated with nimodipine (dissolved in ethanol, 5 µM, 10 µM, 20 µM in final concentration; Sigma, St. Louis, MO, USA) or DMT (dissolved in distilled water, 5 µM, 10 µM, 20 µM and 50 µM in final concentration) on day 6. A stock solution of Baf (Sigma-Aldrich; 160 µM) was used to treat the monocultures (50 nM in final conc.) to inhibit autophagy.

In Project 1 designed to identify the effect of nimodipine the following experimental conditions were established: (i) control (unchallenged, untreated), (ii) activated (challenged with LPS alone) for 24 h, (iii) treated with nimodipine alone (at 5, 10 and 20 µM final concentrations) for 24 h, and (iv) challenged with LPS at the presence of nimodipine (at 5, 10 and 20 µM final concentrations), both LPS and nimodipine applied in combination for 24 h.

Project 2 focusing on the effect of DMT the following experimental conditions were established: (i) control (unchallenged, untreated), (ii) activated (challenged with LPS alone) for 24 h, (iii) treated with DMT alone (at 5, 10, 20 and 50 µM final concentrations) for 24 h, and (iv) challenged with LPS at the presence of DMT (at 5, 10, 20 and 50 µM final concentrations), both LPS and DMT applied in combination for 24 h.

Project 3 the following experimental conditions were established: (i) control (unchallenged, untreated), (ii) activated (challenged with LPS alone) for 24 h, (iii) pre-treated with Baf A1 (50nM) for 3h,) pre-treated with Baf A1 for 3h and activated with LPS for 24h.

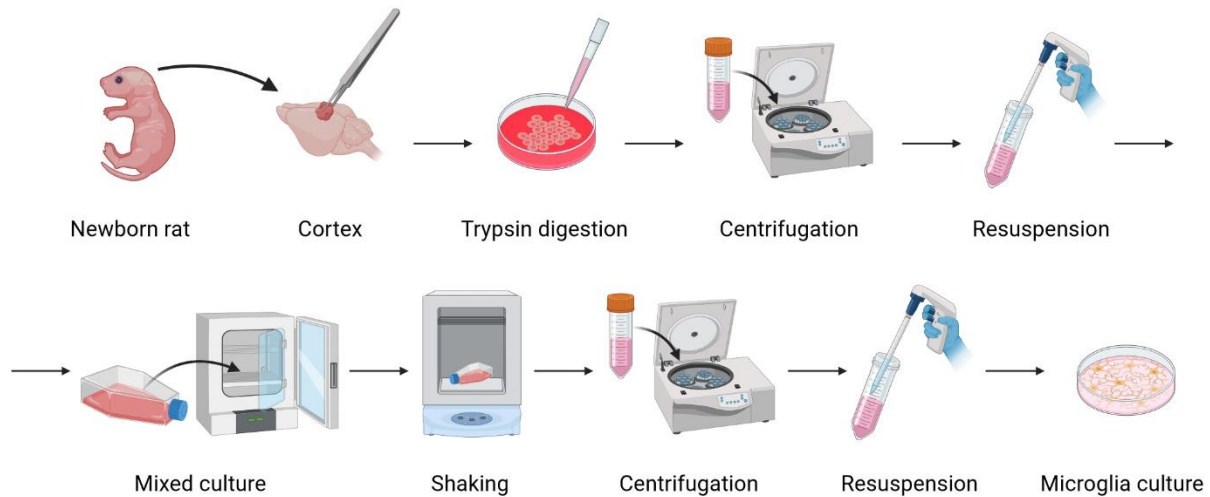


Figure 2.1 Protocol to establish primary microglia monocultures with an initial step of primary mixed cell cultures (reproduced from Pesti et al., 2024).

2.3 Immunohistochemistry

For immunohistochemistry, we used a protocol described previously (Kata et al., 2017). Briefly, primary co-cultures (DIV7) and microglia (subDIV7) monocultures on poly-L-lysine-coated coverslips were used for immunohistochemistry. Cells were fixed in 4% formaldehyde in 0.05 M phosphate buffered saline (PBS, pH 7.4 at RT) for 5 min, then rinsed in 0.05 M PBS for 3 x 5 min. After permeabilization and blocking of nonspecific sites in 0.05 M PBS solution containing 5% normal goat serum (Sigma) and 0.3% Triton X-100 for 60 min at 37°C, the cells on the coverslips were incubated overnight at 4°C with the appropriate primary antibodies (Table 2.1) in 1% heat-inactivated bovine serum albumin (BSA; Sigma) and 0.3% Triton X-100. The cultured cells were washed 3 x 5 min at RT in 0.05 M PBS, then incubated with the appropriate Alexa Fluor fluorochrome-conjugated secondary antibody (Table 2.1) in the above solution, but without Triton X-100, for 2 h at RT in the dark. The cells on the coverslips were washed in 0.05 M PBS for 3 x 5 min at RT, and the nuclei were stained in 0.05 M PBS solution containing 1 mg/ml polyvinylpyrrolidone and 0.5 µl/ml 2-(4-amidinophenyl)-1H-indole-6-carboxamide (DAPI; Thermo Fisher Scientific, Waltham, MA, USA). The coverslips were rinsed in distilled water for 5 minutes, air dried, and mounted on microscope slides in Vectashield mounting medium (Vector Laboratories, Burlingame, CA, USA).

Microscopic images were taken with a LEICA DFC250 camera (Leica Microsystems Wetzlar GmbH, Wetzlar, Germany) attached to a fluorescence microscope (40× magnification, Leica DM LB2, Leica Microsystems CMS GmbH, Wetzlar, Germany).

Table 2.1 Primary and secondary antibodies used for immunocytochemistry and Western blotting

Method	Primary antibody	Company	Final dilution	Secondary antibody	Company	Final dilution
Immuno-cytochemistry	Rabbit anti-Iba1 polyclonal	Abcam, Cambridge, England	1:1000	Alexa Fluor 568 goat anti-rabbit	Invitrogen, Carlsbad, CA, USA	1:1000
	Mouse anti-p62 monoclonal	Abcam, Cambridge, England	1:1000	Alexa Fluor 488 goat anti-mouse	Invitrogen, Carlsbad, CA, USA	1:1000
Western blot	Rabbit anti-Iba1 polyclonal	Abcam, Cambridge, England	1:1000	Anti-rabbit IgG, peroxidase conjugated	Sigma, St. Louis, MO, USA	1:1000
	Mouse anti-p62 monoclonal	Abcam, Cambridge, England	1:300	Anti-mouse IgG, peroxidase conjug.	Sigma, St. Louis, MO, USA	1:1000
	Mouse anti-GAPDH monoclonal	Sigma, St. Louis, USA	1:20000	Anti-mouse IgG, peroxidase conjug.	Sigma, St. Louis, MO, USA	1:1000

2.4 Western blot analysis

Cultured cells from primary co-cultures (DIV7) and microglial (subDIV7) monocultures were harvested with a rubber policeman, homogenized in 50 mM Tris-HCl (pH 7.5) containing 150 mM NaCl, 0.1% Nonidet P40, 0.1% cholic acid, 2 µg/ml leupeptin, 1 µg/ml pepstatin, 2 mM phenylmethylsulfonyl fluoride, and 2 mM EDTA, and centrifuged at 10,000g for 10 min at 4 °C. The pellet was discarded and the protein concentration of the supernatant was determined (Lowry et al., 1951). For quantitative analyses of microglial, neuronal, astrocyte, or oligodendrocyte immunoreactivity, 5-10 µg of protein was separated on a sodium dodecyl sulfate (SDS)-polyacrylamide gel (4-10% stacking gel/resolving gel), transferred to a Hybond-ECL nitrocellulose membrane (Amersham Biosciences, Little Chalfont, Buckinghamshire, England), blocked for 1 hour in 5% nonfat dry milk in Tris-buffered saline (TBS) containing 0.1% Tween-20 and incubated overnight with the appropriate primary antibodies (Table 2.1) as well as the internal control (mouse anti-GAPDH monoclonal antibody). After rinsing 5 times in 0.1% TBS-Tween-20, the membranes were incubated with the appropriate peroxidase-

conjugated secondary antibodies (Table 2.1) for 1 hour and washed 5 times. The enhanced chemiluminescence method (ECL Plus Western blotting detection reagents; Amersham Biosciences) was used to detect immunoreactive bands according to the manufacturer's protocol.

2.5 In vitro phagocytosis assay

The fluid-phase phagocytic capacity of microglial cells in primary co-cultures (DIV7) and microglial (subDIV7) monocultures was determined by uptake of fluorescent microspheres (2 μm diameter; Sigma, St. Louis, MO, USA). Briefly, 1 μL per milliliter of a 2.5% aqueous suspension of fluorescent microspheres was added to the cultures, which were then incubated at 37°C for 60 minutes. The cells were then rinsed five times with 2 mL of PBS to remove any residual fluorescent microspheres bound to the dish or cell surface, and fixed with 4% formaldehyde in 0.05 M PBS (pH 7.4 at RT) (Szabo et al., 2013; Kata et al., 2017). Subsequently, the samples were subjected to immunostaining with Iba1 and DAPI, as described above.

2.6 Enzyme-linked immunosorbent assay (ELISA)

The concentrations of interleukin-10 (IL-10) (ER0033, FineTest) and tumor necrosis factor- α (TNF- α) (ER1393, FineTest) in both primary co-cultures (DIV7) and microglial (subDIV7) monoculture supernatants derived from the Western blot experiments were analyzed using an ELISA kit according to the manufacturer's instructions. An automated microplate reader (Multiskan FC with the software SkanIt RE 5.0, Thermo Scientific) was used to measure optical density (OD) at 450 nm. The concentration of each sample was determined based on the optical density and the concentration of the standard. According to the manufacturer, the overall intra-assay and coefficient of variation were <8% for both IL-10 and TNF- α , and the inter-assay was <10% for both IL-10 and TNF- α .

2.7 NEB mRNA-Library and next generation sequencing

Microglial monocultures were selected for gene expression analysis because the effect of nimodipine on microglial activation was essentially the same in both co-cultures and monocultures, and cell separation was not required for monocultures. Because 10 μM nimodipine was the lowest effective concentration of the drug on microglial activation, we focused the gene expression analysis on this treatment. Total RNA was isolated from the

collected cells with RNeasy Mini Kit (74104 Qiagen) using 1 million cells/sample. Total RNA samples were quantified with Qubit 3.0 Fluorometer (ThermoFisher) and quality checked with Tape Station 4200 instrument using Agilent RNA ScreenTape (Agilent Technologies USA, Cat. No. 5067-5576).

NGS library preparation was carried out using the NEBNext Ultra™ II Directional RNA Library Prep Kit for Illumina (NEB #E7760) with NEBNext Poly(A) mRNA Magnetic Isolation Module (NEB #E7490). After mRNA enrichment, cDNA was generated where a second strand synthesis was done with the dUTP method to retain strand specificity. Finally, double-stranded cDNA was end-prepped and Illumina-specific adaptors were ligated to the cDNA fragments, followed by a final enrichment PCR.

Sequencing ready libraries were quality control checked by Tape Station 4200 instrument using D5000 ScreenTape (Agilent Technologies USA, Cat. No. 5067-5588). Next generation sequencing was carried out on NovaSeq X Plus sequencing system with NextSeq NovaSeq X Series 10B Reagent Kit (300 Cycle) chemistry (Illumina, Inc. USA, 20085594).

2.8 LC-MS/MS analyses

The samples were digested with trypsin according to the Strap micro protocol (<https://files.protefi.com/protocols/s-trap-micro-long-4-7.pdf>, accessed on 23 August 2023). Briefly, samples were supplemented with 20% SDS and dried down then redissolved in 50 mM TEAB to give a final SDS concentration of 5% followed by reduction using TCEP (Tris(2-carboxyethyl)phosphine) for 15 min at 37°C, and alkylation with MMTS (S-methyl methanethiosulfonate) for 15 min at room temperature before digesting with MS-grade trypsin (Pierce Biotechnology, Rockford, IL, USA) for 2h at 47 °C. 10% of the resulting peptide mixtures were loaded onto C18 EvoTips (Evosep) for LC-MS analysis. Reversed-phase separation of the peptides was performed using an Evosep One HPLC (Evosep) applying the „15 SPD” 88-min gradient using a “performance” column packed with 1.5 µm particles of ReproSil-Pur C18 beads (length: 150mm, internal diameter: 0.15mm), followed by data-dependent MS/MS acquisition using an Orbitrap Fusion Lumos Tribrid (Thermo Scientific) mass spectrometer equipped with a FAIMS Pro ion mobility device (Thermo Scientific). Data were collected using two compensation voltages (-70 and -50 V) in alternating 1.5s cycles. All data were acquired with high resolution (120000 and 15000 for MS and MS/MS data, respectively) in the Orbitrap analyzer. AGC target was set at 400,000 and 50,000 for MS and MS/MS acquisition, respectively; MS2 intensity threshold was set to 50,000, higher-energy

collision dissociation (HCD) activation was applied using stepped collision energies of NCE=32 and 35. Dynamic exclusion was enabled (exclusion time: 60s).

2.9 Image analysis

Digital images of the Iba1-labeled immunocytochemical preparations were captured using a LEICA DFC250 camera (Leica Microsystems Wetzlar GmbH, Wetzlar, Germany) attached to a fluorescence microscope (Leica DM LB2, Leica Microsystems CMS GmbH, Wetzlar, Germany) and LAS X Application Suite (Leica Microsystems CMS GmbH, Wetzlar, Germany). To determine the purity of microglial cells, DAPI-labeled nuclei of Iba1-immunopositive cells were counted. In cell cultures, at least two coverslips from each experiment were analyzed, with approximately 20 randomly selected cells per coverslip in three separate experiments. Microglial cell silhouettes were obtained by converting the raw digital files of Iba1-immunoreactive cells captured by fluorescence microscopy into binary files using Adobe Photoshop CS3 software (Adobe Systems, Inc., San Jose, CA, USA). After binary conversion, cell perimeter and area of individual cells were measured in ImageJ (National Institutes of Health, Bethesda, MD, USA) and the TI reflecting the degree of process extension was calculated as follows: $\text{perimeter}^2/\text{area} * 4\pi$ as previously described (Fujita et al., 1996). A total of 420 cell silhouettes were analyzed in nimodipine and 210 in DMT experiment.

To measure phagocytic activity, cells were labeled with phagocytosed microbeads and identified with Iba1 immunocytochemistry. The microbeads in the cytoplasm were counted. Twenty non-overlapping random fields were captured using a fluorescence microscope with a 40x objective (Leica DMLB epifluorescence microscope), and the microbead load of a total of 100 cells in each culture was evaluated using the ImageJ cell counter plugin (National Institutes of Health, Bethesda, MD, USA). The mean microbead count of 100 cells was taken as a single value representing each culture.

Gray-scale digital images of the immunoblots were obtained by scanning the autoradiographic films with a desktop scanner (Epson 430 Perfection V750 PRO; Seiko Epson Corp., Suwa, Japan). Images were scanned and processed with identical settings to allow comparison of blots from different samples. The bands were outlined and analyzed by densitometry using ImageJ (National Institutes of Health, Bethesda, MD, USA). Immunoreactive densities of equally loaded lanes were quantified as we previously reported (Kata et al., 2016, 2017). Samples were normalized to the densities of internal controls (GAPDH) and presented as % of untreated controls.

2.10 Statistical analysis

Statistical comparisons for microglial morphology, Western blot, phagocytic activity, and ELISA assay were performed using GraphPad Prism 8.0 (Windows, GraphPad Software, San Diego, California USA, www.graphpad.com). Normality of data distribution was determined by the Shapiro-Wilk test. In case of normal distribution of data, one-way analysis of variance (ANOVA) followed by Tukey's multiple comparison test was used for statistical analysis, and data were presented as mean \pm SD in bar graphs. In case of non-normal distribution of data, Kruskal-Wallis test followed by Dunn's multiple comparison was used and data were presented in box plots. The significance level was set at $p < 0.05$.

For the processing of RNA-Sequencing data, the quality of the pair-ended reads was performed using FastQC (0.12.1) (Andrews, 2010), while adapters and low-quality bases were trimmed using FASTP (0.23.4) (Chen et al., 2018). The filtered reads were aligned to the *Rattus norvegicus* genome (NCBI: GRCr8) using the splice-aware aligner, STAR (2.5.2b) (Dobin et al., 2013), and quantified with FeatureCounts (v.2.0.6) (Liao et al., 2014). For the downstream analysis, only genes with a CPM (counts per million) greater than 2 in at least three samples were retained. The filtered samples were then normalized using the TMM (Trimmed Mean of M-values) method implemented in edgeR's `calcNormFactors` (v.4.0.16) function (Robinson et al., 2010). Differential gene expression analysis was performed using limma-voom (Law et al., 2014).

PCA and hierarchical clustering were used to examine the similarities between samples and identify potential outliers. Differently expressed genes (DEGs) were identified for the following comparisons: (i) LPS vs. Control, (ii) LPS+nimodipine vs. Control, and (iii) LPS+nimodipine vs. LPS. In each comparison, DEGs were defined as those with a log₂ fold change greater than 1 and an adjusted p-value < 0.05 .

To assess the effects of different treatments on gene expression, we selected genes from various pathways and analyzed their expression changes. Log Fold Change and p-values were used to evaluate the differential expression of these genes across comparisons. We identified significantly upregulated and downregulated genes. Additionally, heatmaps were generated for each pathway to provide a detailed view of expression patterns. The complete results of this analysis, including all significant genes, are available in the supplementary materials.

Peptide identification and quantitation were done using the Proteome Discoverer software (Thermo Scientific, v3.0). Peptides and proteins were identified with Sequest HT search engine using the rat (sp_canonical TaxID=10116, v2023-06-28, 8178 sequences) and bovine

(sp_canonical TaxID=9913, v2022-12-14, 6034 sequences) subsets of the Swissprot protein database. Trypsin was specified as enzyme allowing up to two missed cleavage sites. Mass accuracy was set at 5 ppm and 0.02 Da for precursor and fragment ions, respectively. Constant modification was methylthio on Cys residues. Acetylation and/or loss of Met on protein N-terminus, oxidation of Met and cyclization of peptide N-terminal Gln were set as variable modifications allowing up to 4 variable modifications per peptide. Label free quantitation was performed using precursor MS signal intensities. Unique and razor peptides were considered for pairwise ratio based comparison of the sample groups (acceptance parameters: Sequest HT Xcorr>1, S/N in MS spectra >5, retention time window: 5 min, minimum replicate feature≥50%). Proteins identified with high confidence showing $|\log_2\text{FoldChange}|>1$ (adjusted p-Value≤0.05 using background-based t-test) were accepted as differently expressed.

3. Results

3.1 Nimodipine mitigates microglia activation

3.1.1 Nimodipine effect on microglial morphological phenotype

The morphological phenotype of microglial cells can be used to infer their activation state. They show a ramified phenotype in the resting state, whereas upon activation their branches shorten, and they assume a round amoeboid cell shape. In mixed cell culture, untreated control microglia cells take on a ramified cell shape with small pseudopodia with TI~2.6 close to resting state (Fig 3.1A-B). In pure microglia culture, the control group had more branches and were even more ramified with TI ~3.2 (Fig. 3.1C-D) than in co-cultures. Upon activation with LPS, the TI of microglia cells in both co- cultures (TI~1.4) and monocultures (TI~1.5) was significantly reduced, indicating an activated amoeboid morphological phenotype (Fig. 3). When different concentrations of nimodipine (5, 10, 20 μM) were added to the non-activated cultures, more microspikes (filopodia) appeared in both co-cultures and monocultures (Fig. 3.1A, C), which increased the TI, although the change was not significant (Fig. 3.1B, D). Addition of nimodipine to LPS-activated microglia cells increased the TI of the cells in both co- and monocultures. In particular, concentrations of 10 and 20 μM were effective in increasing the ramification close to the branches of the control group (Fig. 3.1). This suggests that nimodipine is able to affect the morphological phenotype changes of microglial cells.

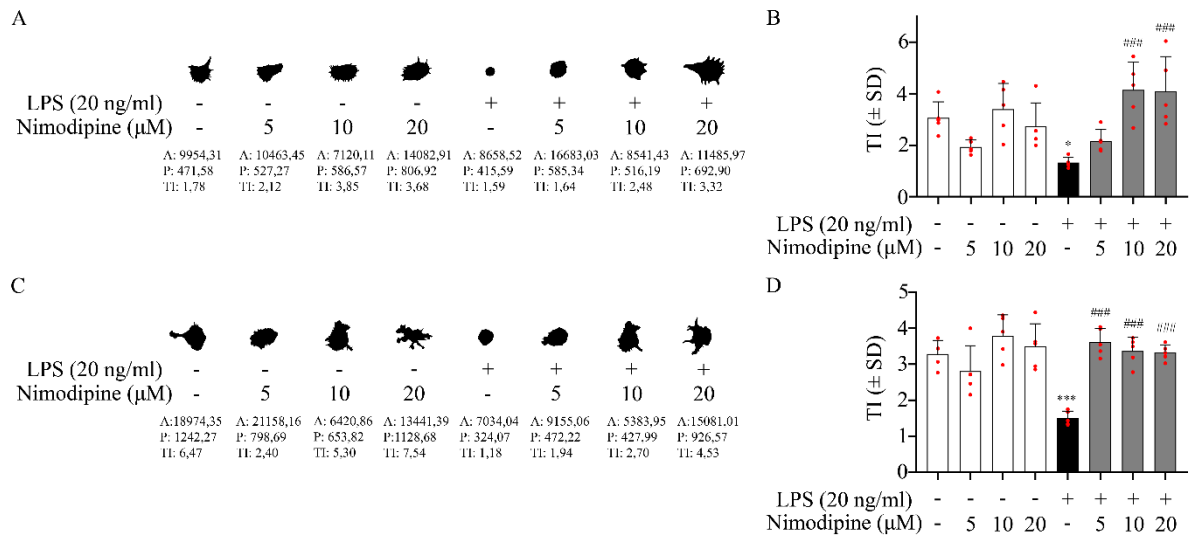


Figure 3.1 Microglial morphology in co-cultures (A-B) and microglia monocultures (C-D). **A**, Iba1-positive cell masks representative of microglia in co-cultures (DIV7). **B**, Microglial transformation index (TI) calculated for each experimental condition in co-cultures. **C**, Iba1-positive cell masks representative of microglia in monocultures (subDIV7). **D**, Transformation index (TI) calculated for each experimental condition in microglia monocultures. In A and C, the values are given below the masks: A, area; P, perimeter; TI, transformation index. In B and D, data were obtained as follows: The morphological phenotype of 15 randomly selected microglia per culture were evaluated and the average was taken as a single data point. Five cell cultures were analysed in each of the 8 experimental groups. Data are presented as mean \pm SD; red spheres represent individual values in each condition (n=15/experimental condition). Normality of the data distribution was determined by the Shapiro-Wilk test (B, $p=0.658$; D, $p=0.374$). Data were analysed by one-way analysis of variance (ANOVA) (B, $f=6.310$, $p<0.001^{****}$, D, $f=7.829$, $p<0.001^{****}$) followed by Tukey's multiple comparison (B, $p<0.05^*$ vs. absolute control; $p<0.001^{###}$ vs. LPS alone; D, $p<0.05^{***}$ vs. absolute control; $p<0.001^{###}$ vs. LPS alone).

3.1.2 Nimodipine effect on microglial functional phenotype

Non-activated microglia cells at rest have low phagocytosis while they engulf few microbeads in both co- and monocultures. The use of nimodipine treatment at different concentrations in non-activated cultures did not cause any change in the phagocytosis, which remained at the same low level of phagocytosed microbeads. LPS activation significantly increased the microglial phagocytic activity, which was shown by an increased number of engulfed microbeads in both co- and monocultures. Treatment of LPS-activated cells with nimodipine significantly reduced phagocytosis to near control levels in both co- and monoculture (Fig. 3.2).

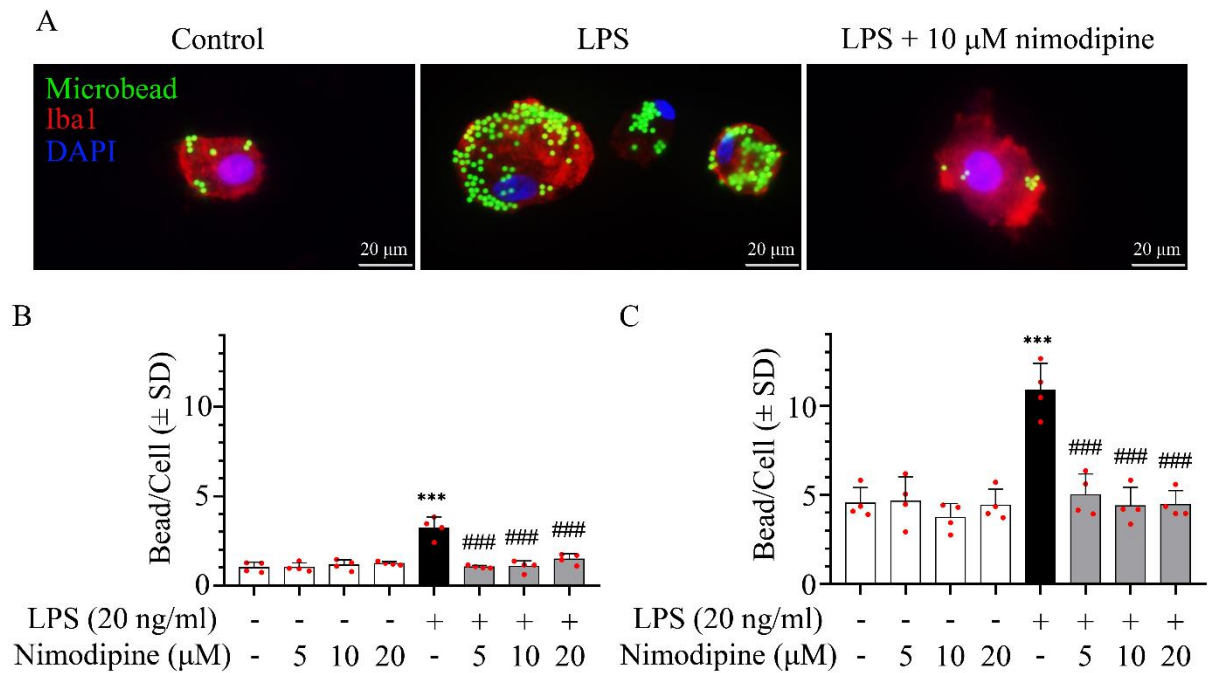


Figure 3.2 Microglial phagocytic activity in co- and monoculture. **A**, Representative fluorescence microscopic images of Iba1-labeled microglia in monocultures. Fluorescent microbeads in their cytoplasm indicate increased phagocytic activity after LPS activation, which was reduced by nimodipine. **B**, Phagocytotic activity of microglia quantified in co-cultures. **C**, Phagocytotic activity quantified in microglial monocultures. In **B** and **C**, data are presented as mean±SD; red spheres represent individual cultures (mean of 100 cells analyzed in each culture) in each group. Normality of data distribution was determined by Shapiro-Wilk test (**B**, $p=0.259$; **C**, $p=0.216$). Data were analyzed by one-way analysis of variance (ANOVA) ($f=49.640$, $p<0.001^{***}$) followed by Tukey's multiple comparison ($p<0.001^{***}$ vs. absolute control; $p<0.001^{###}$ vs. LPS alone).

In microglia, the expression of *iba1* can be used to determine the activation state of the cell (Ito et al., 1998). Western blot analysis showed, when cells were activated with LPS, *Iba1* expression was significantly increased compared to a non-activated control group in both co- and monocultures (Fig. 3.3). Nimodipine treatment in non-activated cultures does not cause a shift in *Iba1* expression. In contrast, when added to LPS-activated cultures, its concentration-dependently reduced *Iba1* protein levels and reached significance at 10 and 20 μM concentrations in microglia co-cultures (Fig. 3.3B). In microglia monoculture, *iba1* levels were reduced to near control levels at all three concentrations (Fig. 3.3D).

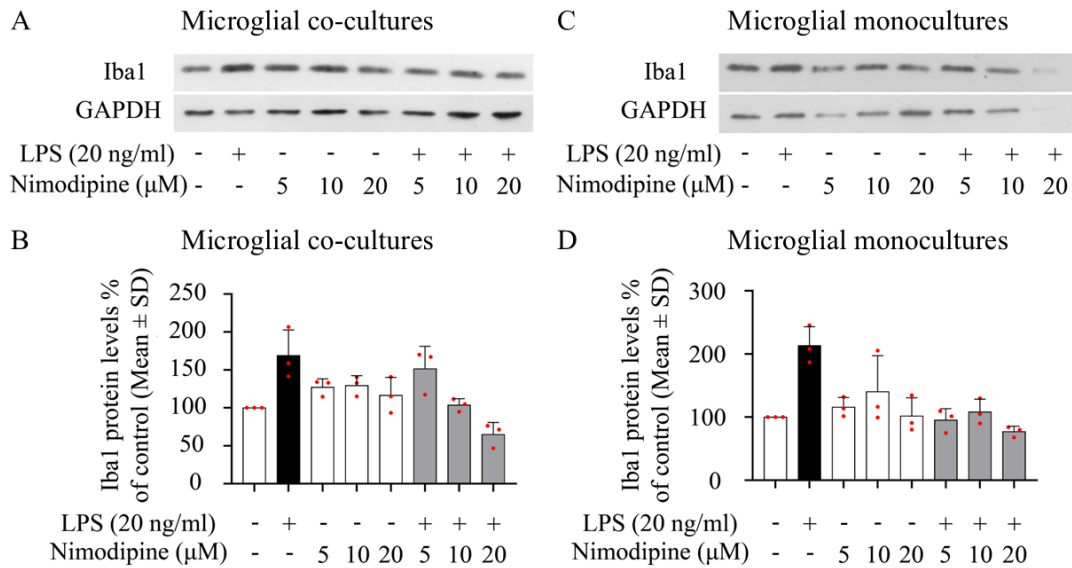


Figure 3.3 Microglial Iba1 protein levels in co-cultures (A-B) and microglial monocultures (C-D). **A,** Representative Western blot images for Iba1 and GAPDH from co-cultures. **B,** Iba1 protein levels quantified in co-cultures. **C,** Representative Western blot images for Iba1 and GAPDH from microglial monocultures. **D,** Iba1 protein levels quantified in microglia monocultures. In A and C, images were scanned and processed with identical settings to allow comparisons between Western blots from different samples. In B and D, data are integrated optical density values relative to control, and the descriptive statistics present data as mean±SD. Red spheres indicate individual values (n=3) in each group.

Activated microglia cells are characterized by the production of different cytokines. Depending on their phenotype, these can be pro-inflammatory or anti-inflammatory cytokines. We investigated whether nimodipine affects the amount of pro-inflammatory cytokine TNF- α and anti-inflammatory cytokine IL-10 secretion by microglia cells in the culture medium. The use of low concentrations of LPS (20 ng/ml) did not result in any change in the amount of IL-10 in either co- or monocultures. Nimodipine was observed to have no significant impact on IL-10 levels, irrespective of whether the cultures were non-activated or activated. Low-dose LPS stimulation did not result in a statistically significant alteration in the TNF- α concentration measured at 24 hours (peak values had been previously measured at 6 h, Kata et al., 2016), although a discernible tendency towards an increase was observed in both co-cultures and monocultures (Fig 3.4). It was observed that nimodipine exerted no effect on non-activated cultures. However, at a concentration of 20 μ M, nimodipine was observed to reduce TNF- α concentrations in LPS-activated co-cultures to control levels (Fig 3.4A). In LPS-activated monocultures, nimodipine produced a stepwise reduction in TNF- α levels in a concentration-dependent manner, although this reduction did not achieve statistical significance (Fig 3.4B).

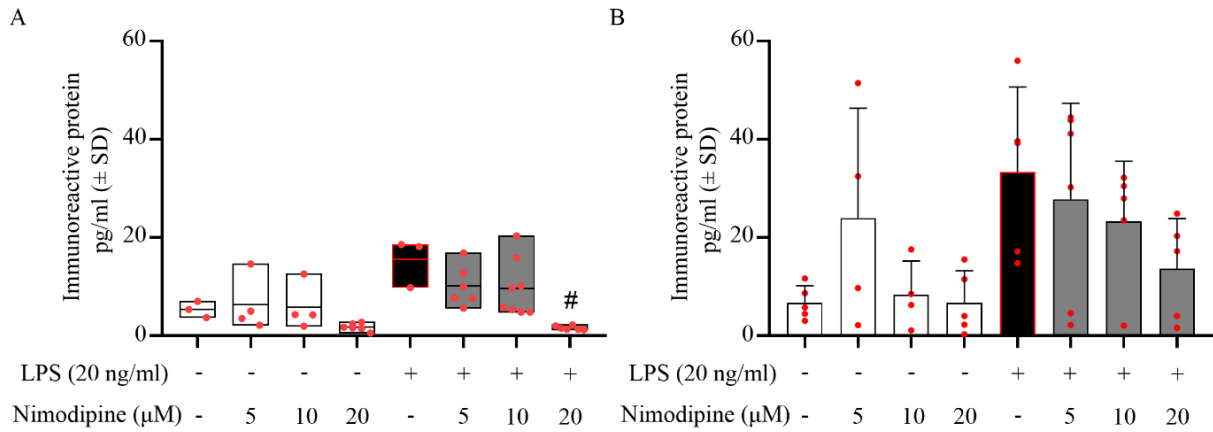


Figure 3.4 Tumor necrosis factor- α secretion (TNF- α) level in culture medium. **A**, Quantitative analysis of TNF- α concentration in the co-cultures by ELISA. **B**, Quantitative analysis of TNF- α levels in the monoculture medium by ELISA. Data are presented as mean \pm SD; red spheres represent individual values in each group. Normality of data distribution was determined by Shapiro-Wilk test (A, $p=0.025$; B, $p=0.175$). Data were analyzed by Kruskal-Wallis test ($p<0.0002$) followed by Dunn's multiple comparison ($p<0.05^{\#}$ vs. LPS alone) (A) or one-way analysis of variance (ANOVA) ($f=2.783$, $p=0.0229^*$) followed by Tukey's multiple comparison (B).

3.1.3 Potential mechanisms of nimodipine effect on activated microglia

Subsequently, next-generation RNA sequencing was performed on microglial monocultures only. The analysis identified a total of 13,866 genes, of which 9,720 were found to be differentially expressed (DEGs) as a result of LPS activation or in combination with nimodipine treatment (Fig. 3.5).

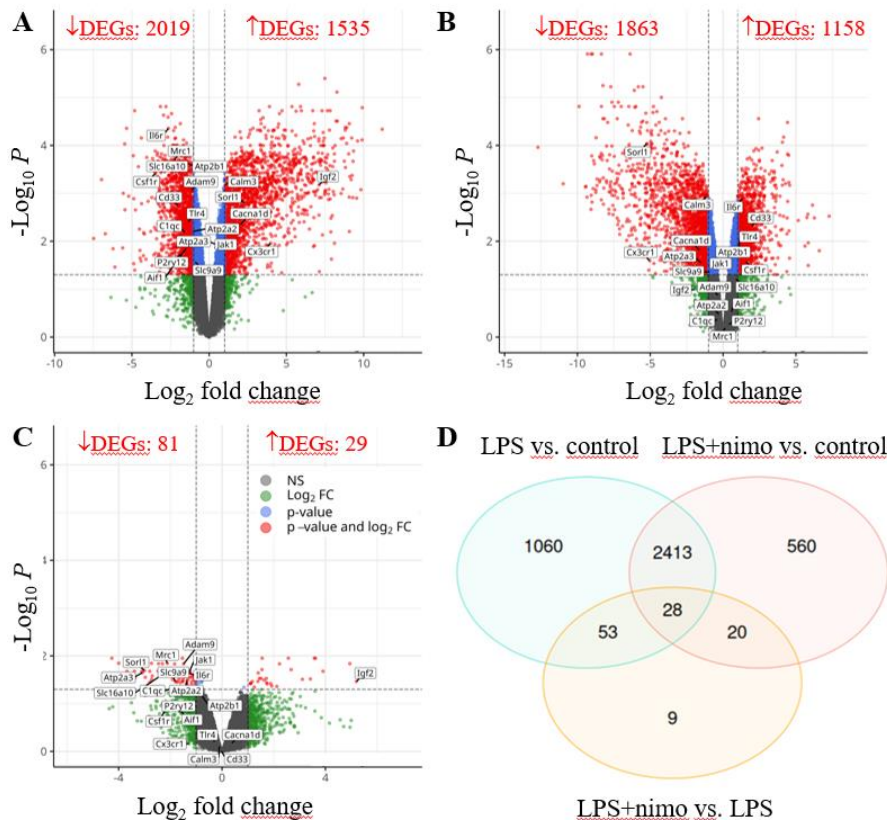


Figure 3.5 Microglia monocultures transcriptome. Volcano plots depict Log₂ fold changes and $-\text{Log}_{10}$ of the adjusted p-value per gene comparing LPS vs. control (A), LPS+nimodipine treatment vs. control (B) and LPS+nimodipine treatment vs. LPS alone (C). Venn diagram shows the overlap of differentially expressed genes (DEGs) in the three experimental conditions (D). Cutoff values are $\text{Log}_2\text{FC}=1$ and $p=0.05$.

To increase the previously described phagocytic activity, we investigated which genes are altered by LPS. The results showed that the expression of several genes involved in phagocytosis was increased (e.g. Mertk, Trem1, Cd14, Cd33, Cd68, Ms4a4a) (Fig. 3.6).

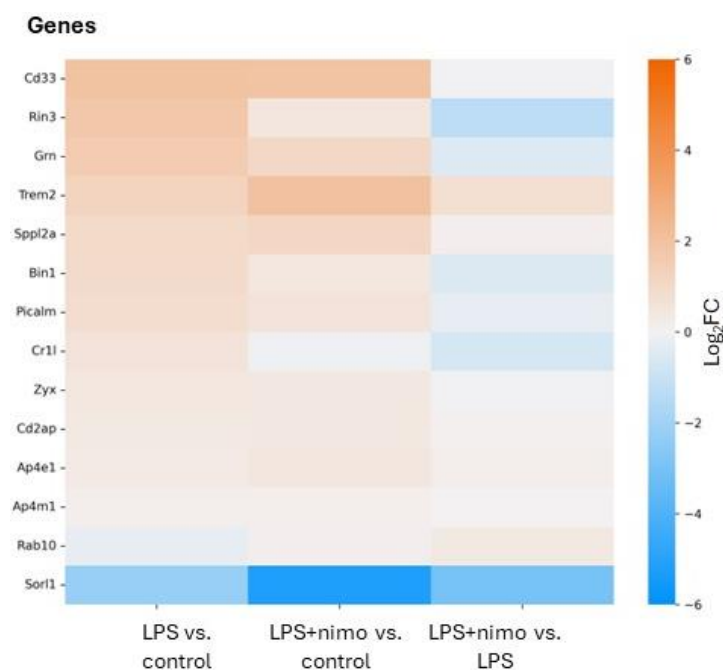


Figure 3.6 Heat map of differentially expressed genes (DEGs) of markers of phagocytosis. The heatmap shows downregulated proteins in blue and upregulated proteins in red. The first column shows the protein change in response to LPS compared to the control. The middle column shows the protein change in response to nimodipine and LPS treatment compared to the control. The last column shows the change in protein levels after nimodipine and LPS treatment compared to the LPS. Selection criteria: $-1 > \text{Log}_2\text{FC} > 1$ and $\text{adj.}p < 0.05$.

Autophagy is involved in maintaining cellular homeostasis by degrading dysfunctional organelles and damaged proteins and may suppress inflammation. The expression of genes that are directly involved in macroautophagy was not altered by LPS activation, but the expression of proteins that are indirectly involved in macroautophagy regulation, such as Wdfy3 and Dnajc16, were significantly increased (Table 3.1).

Table 3.1 Changes in gene expression of markers of autophagy in primary microglia monocultures. Change in mRNA expression is expressed as Log₂FC (adjusted $p < 0.05^*$); Cells showing data $\text{Log}_2\text{FC} > 1$ and adjusted $p < 0.05^*$ are colour coded.

Function	Gene	Protein	LPS vs. Control	LPS+nimo vs. Control	nimo+LPS vs. LPS
Auto-phagy	Wdfy3	WD Repeat And FYVE Domain Containing 3	1.512207***	0.413049	-1.099157*
	Dnajc16	DnaJ homolog subfamily C member 16	1.080475**	-0.014745	-1.095221*

Change in mRNA expression is expressed as Log₂FC (adjusted $p < 0.001^{***}$, $p < 0.01^{**}$, $p < 0.05^*$); Cells showing data $\text{Log}_2\text{FC} > 1$ and adjusted $p < 0.05^*$ are color-coded.

Upregulated	Downregulated	No change
-------------	---------------	-----------

Because microglial activation is associated with an increase in intracellular Ca^{2+} levels, we investigated the role of nimodipine, which is a calcium channel blocker. The increase in intracellular Ca^{2+} levels can occur via Ca^{2+} from the extracellular space or from intracellular

organelles. In this study, we have investigated the transcripts of ion channels and receptors involved in cellular Ca²⁺ currents. The results obtained indicate that the expression of the TRPM2 channel and the purinergic receptor P2X4 was increased by LPS, suggesting an elevated influx of Ca²⁺ via these routes into the cytoplasm. Conversely, the expression of genes encoding VGCCs was found to be downregulated by LPS (Table 3.2).

Table 3.2 Changes in gene expression of calcium channels and calcium binding proteins in primary microglia monocultures.

		Gene	LPS vs. Control	LPS+nimo vs. Control	LPS+nimo vs. LPS	
Voltage-gated channels	Cav2.1 (P/Q type)	Cacna1a	-0.721915872789663*	-0.394759125925211	0.327156746864452	
	Cav2.2 (N type)	Cacna1b	0.601297994808163	0.713859465111638	0.112561470303475	
	Cav1.2 (L type)	Cacna1c	-0.257819824060129	0.35183185448832	0.609651678548449	
	Cav1.3 (L type)	Cacna1d	-2.00822688139661**	-1.62905113340612*	0.379175747990492	
	Cav2.3 (R type)	Cacna1e	-6.3552850288316***	-4.19331267255001**	2.16197235628159	
	Cav3.1 (T type)	Cacna1g	-1.32157896986769**	-1.44464705890393**	-0.123068089036233	
	Cav3.2(T type)	Cacna1h	-4.33325238284772***	-3.1829834837996***	1.15026889904812	
Ligand gated ion channels	NMDA glutamate receptor subunits	Grina	-0.357529042629293	0.253214953714641	0.610743996343934	
		Grin3a	-5.77352221589529***	-3.80861702126573**	1.96490519462956	
		Grin3b	0.582217177241407*	0.371345289222701	-0.210871888018707	
		Grin2d	-0.408768400298131	-0.44639696994924	-0.0376285696511087	
	AMPA glutamate receptor subunits	Gria1	-8.75606903233361***	-5.18684203173138***	3.56922700060223*	
		Gria2	-3.93856435597708**	-7.44506670377234***	-3.50650234779526	
		Gria3	0.475310320110989	0.027454174286655	-0.447856145824334	
	Ionotropic purinergic receptors	P2rx4	1.16350452669922**	0.426599458092863	-0.736905068606362	
		P2rx5	1.68477934816561	1.99357218113975	0.308792832974141	
		P2rx7	-0.505257619840301	0.558233801321241	1.06349142116154	
TRP channels	TRPM2	Trpm2	1.85754869589203**	0.935080263653063	-0.922468432238963	
	TRPM7	Trpm7	-0.0819432312635966	-0.198334452069794	-0.116391220806197	
	TRPV1	Trpv1	0.900433026810162	0.820543018599472	-0.0798900082106896	
Calcium release-activated calcium channel	Orai1	0.252669103240033	1.01476562827709	0.762096525037054		
Endoplasmic reticulum	Ryr	Ryr2	-3.95910216286549	-4.64064723872193*	-0.68154507585644	
		Ryr3	-2.46774743744091**	-1.41150968208879*	1.05623775535212	
	Ip3R	Itpr1	-1.10159739033999*	-1.39565561008842**	-0.294058219748431	
		Itpr2	0.980746574724361**	-0.284135727111085	-1.26488230183545*	
		Itpr3	-0.983122359165874*	-1.21479577040357*	-0.231673411237698	
	SERCA	Atp2a2	-1.07178051722827**	-0.283096347019999	-1.35487686424827*	
Atp2a3		1.58865638348008*	-1.48893377879525*	-3.07759016227533*		
Mito-chondrium	Mitochondrial	Mcu	-0.642371381969961*	-0.49943362821703*	0.142937753752931	
	Calcium Uniporter subunits	Mcub	-0.0008077829090709	0.449721223978286	0.450529006887356	
		Mcur1	0.0439527753552664	-0.473506798812516	-0.517459574167783	
	NCX, member b1	Slc8b1	1.51580685006666**	1.31357412424222**	-0.202232725824439	
Calcium binding proteins	lba1	Aif1	1.4997933728521*	0.566155775893205	-0.933637596958893	
		Calmodulins	Calm1	-0.213026232205602	0.462631866377775	0.675658098583376
			Calm2	-0.409379611126846	-0.388512774095398	0.0208668370314484
	Calm3		-1.03474192679683**	-1.13801936306392**	-0.10327743626709	
	Calcineurin subunits	Ppp3ca	0.616960641546393	0.615587845288454	-0.0013727962579386	
		Ppp3cb	-0.349562509159074	-0.169122368507913	0.180440140651161	
		Ppp3cc	-0.699421538720193*	-0.344551900286994	0.354869638433198	
		Ppp3r1	-0.156344491068309	-0.0849962325163665	0.0713482585519429	
	Rcan1	-0.005260155475689	-0.407043447858539	-0.401783292382849		

Change in mRNA expression is expressed as Log₂FC (adjusted p<0.001***, p<0.01**, p<0.05*); Cells showing data Log₂FC>1 and adjusted p<0.05* are color-coded.

Upregulated	Downregulated	No change
-------------	---------------	-----------

This finding led to the formulation of a hypothesis that the downregulation of VGCCs may serve as a compensatory mechanism for the increased expression of TRPM2 and the P2X4 purinergic receptor. Comparison of LPS-challenged microglia with the control showed that RyR genes (Ryr2-3) along with the IP3R genes (Itpr1-3) were downregulated. The SERCA Ca^{2+} pump, located within the endoplasmic reticulum, functions to sequester and accumulate Ca^{2+} within this compartment. Genes encoding SERCA (Atp2a2 and Atp2a3) were remarkably upregulated by exposure to LPS. Consequently, it is hypothesized that SERCA pumps function to normalize elevated intracellular Ca^{2+} concentrations associated with microglial activation through their augmented expression.

In the primary microglial monocultures examined, the combination of nimodipine and LPS led to changes in the expression of 110 genes when compared to the effects of LPS alone (refer to Figures 3.5 and 3.7). Among these differentially expressed genes (DEGs), 29 exhibited upregulation, while 81 showed downregulation. It is important to highlight that the influence of nimodipine was contrary to that of LPS (Fig. 3.7). The analysis of these 110 genes indicated that at least 20 were linked to the microglial immune response, 7 were associated with cell adhesion, and 2 were related to the regulation of autophagy (Fig. 3.7), along with 4 that played a role in intracellular calcium homeostasis.

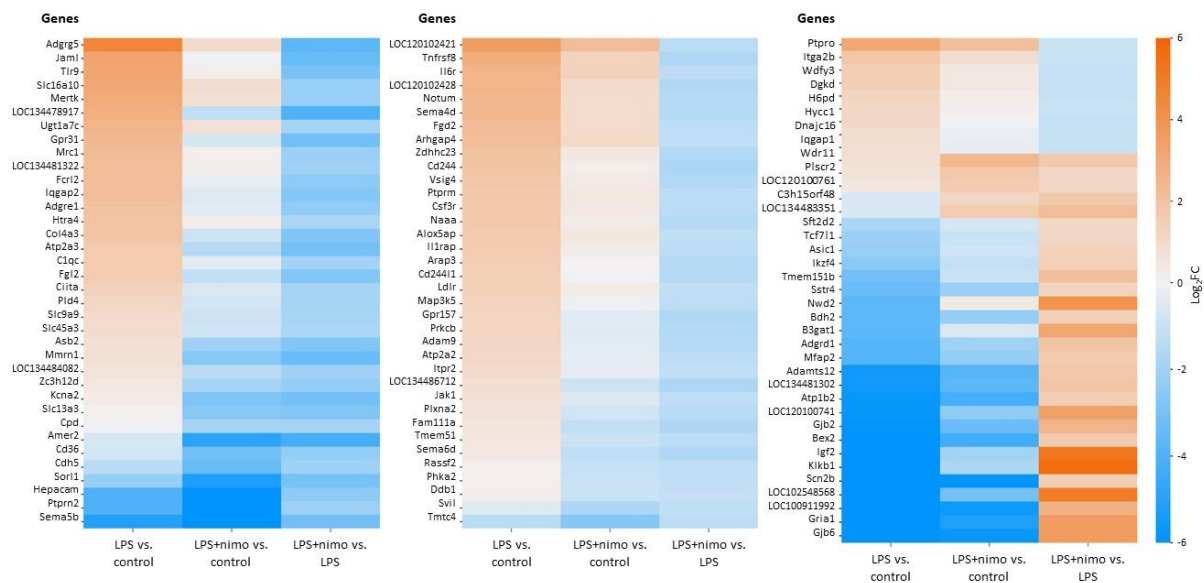


Figure 3.7 Heat maps of differentially expressed genes (DEGs) selected for significant change by nimodipine treatment (LPS+nimodipine) compared to LPS challenge alone (selection criteria: $-1 > \text{Log}_2\text{FC} > 1$ and $\text{adj.}p < 0.05$).

3.2 DMT modulates microglial activation

3.2.1 DMT effect on microglial morphological phenotype

DMT alone at all concentrations showed a tendency to augment the resting state of microglia, as indicated by an increased transformation index, which also reached statistical difference at the 10 μM concentration (Fig. 3.8). The low transformation index values observed with LPS treatment were not altered by 5 and 10 μM DMT treatments, but 20 and 50 μM DMT treatments significantly increased the transformation index values, thus shifting microglia cells towards more ramified cell types.

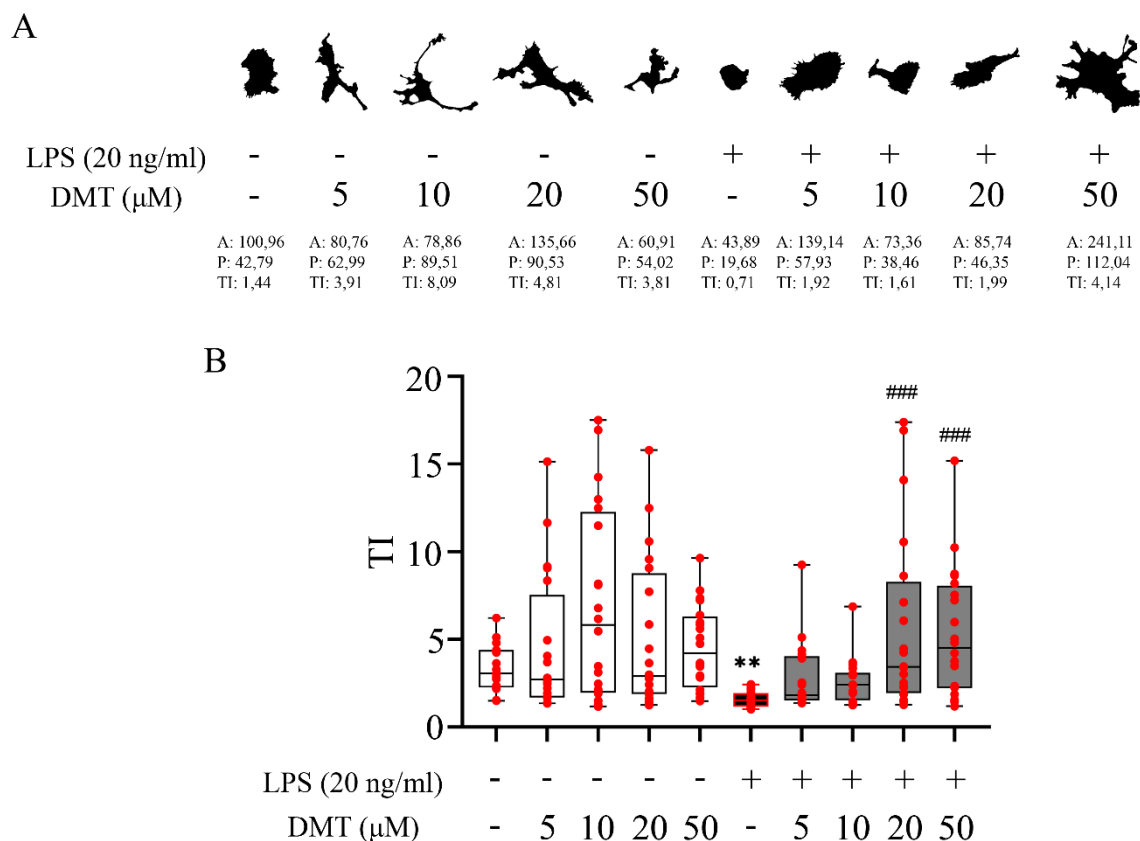


Figure 3.8 Microglial morphology microglia monocultures (A-B). **A**, Iba1-positive cell masks representative of microglia in monocultures (subDIV7). **B**, Transformation index (TI) calculated for each experimental condition in microglia monocultures. In A the values are given below the masks: A, area; P, perimeter; TI, transformation index. In B data are presented as min to max in box plots; red spheres represent individual values in each condition (n=21). Normality of the data distribution was determined by the Shapiro-Wilk test (B: $p < 0.001$). Data were analyzed by Kruskal-Wallis test (B, $p < 0.001^{***}$) followed by Dunn's multiple comparison ($p < 0.01^{**}$ vs. absolute control; $p < 0.001^{###}$ vs. LPS alone).

3.2.2 DMT effect on microglial functional phenotype

During DMT treatment the proportion of phagocytic and non-phagocytic cells in each culture was determined. In the control cultures, the ratio of phagocytic to non-phagocytic cells was close to 50-50%. LPS treatment increased the proportion of phagocytic cells (67%) at the

expense of non-phagocytic cells (33%) (Fig. 3.9). DMT administered with LPS at concentrations of 20 and 50 μM reduced phagocytotic activity to control level (Fig. 3.9).

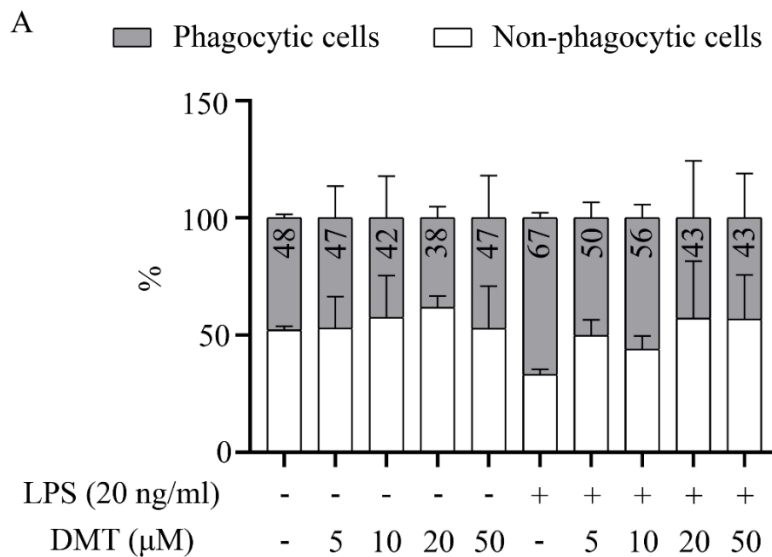


Figure 3.9 Phagocytic ratio of microglial cells in different treatments. The bar chart illustrates the proportion of phagocytic cells in grey, with the non-phagocytic cells represented by white.

LPS activation caused a significant elevation of Iba1 protein expression compared to absolute control. DMT did not reverse the LPS-induced Iba1 expression. In fact, DMT alone showed a tendency to upregulate Iba1 (Fig. 3.10B).

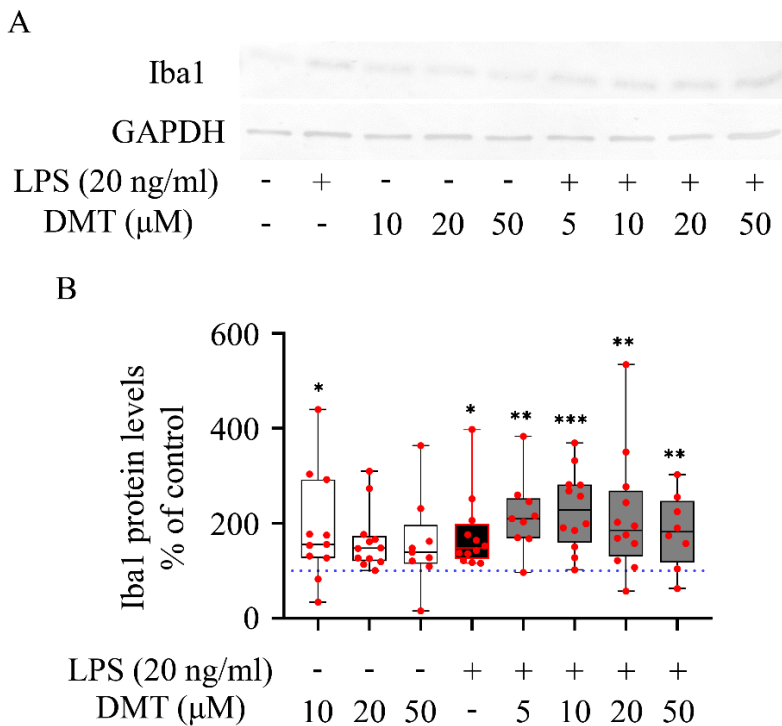


Figure 3.10 Microglial Iba1 protein levels in monocultures (A-B). A, Representative Western blot images for Iba1 and GAPDH from monocultures. B, Iba1 protein levels quantified in microglia monocultures. In A, images were scanned and processed with identical settings to allow comparisons between Western blots from different samples. In B, data are integrated optical density values relative to control (horizontal dotted line) and are presented as min to max in box plots (n=12). Red spheres indicate individual values in each group. Normality of data distribution was determined by Shapiro-Wilk test (B: $p < 0.001$). Data were analyzed by Kruskal-Wallis test (B, $p = 0.0002^{***}$) followed by Dunn's multiple comparison ($p < 0.05^*$, $p < 0.01^{**}$, $p < 0.001^{***}$ vs. absolute control).

3.2.3 Proteomic changes in microglia in response to DMT treatment

Proteomic analyses identified a total of 2793 proteins, of which 244 proteins were altered (Fig. 3.11A). Comparisons between groups showed that LPS resulted in upregulation of 111 proteins and downregulation of 33 proteins compared to control (Fig. 3.11B). The addition of DMT to LPS resulted in the upregulation of 76 proteins and the downregulation of 86 proteins compared to the control culture, indicating the effect of DMT (Fig. 3.11C). Finally, co-administration of DMT and LPS resulted in upregulation of 21 proteins and downregulation of 84 proteins compared to LPS (Fig. 3.11D).

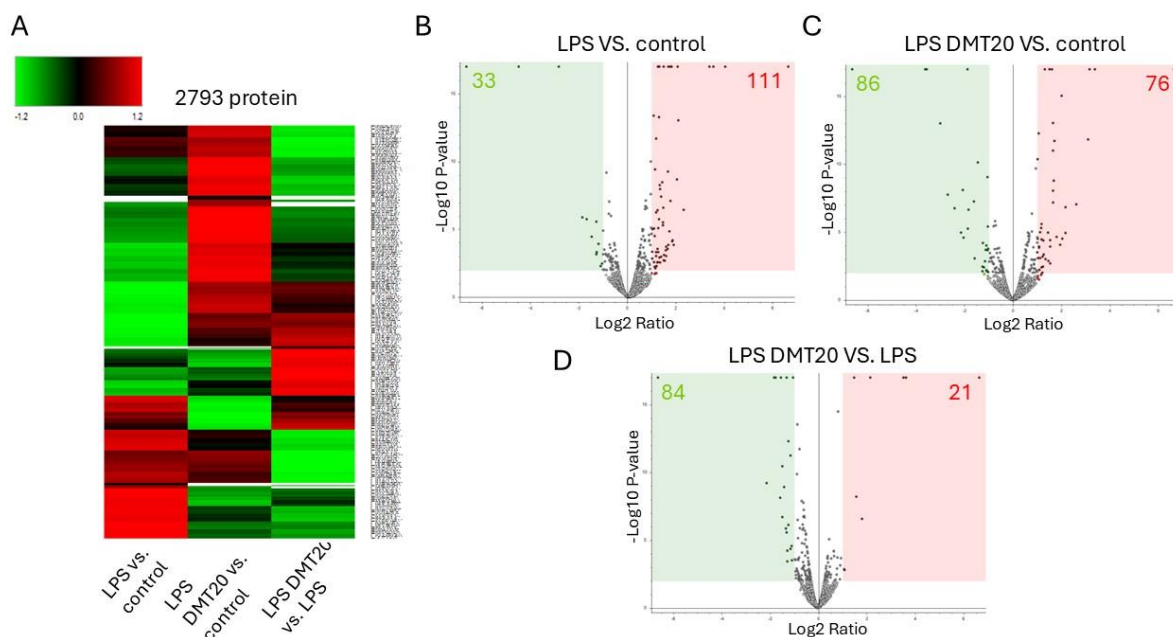


Figure 3.11 Results of proteomic studies. Changes in microglial protein expression are summarized in a heatmap (red: upregulation, green: downregulation) (A). Volcan plots of data from protein expression analysis show significantly downregulated (green background) and upregulated (red background) proteins in pairwise group comparisons: LPS vs. Control (B), LPS+DMT vs. Control (C) LPS+DMT vs. LPS (D). The horizontal axis represents the protein quantitative change (\log_2) and the vertical axis represents the statistical P-value of the change ($-\log_{10}$).

We then searched for proteins whose expression was altered by LPS and then reversed by the addition of DMT. Eight proteins were identified that were upregulated by LSP and then DMT reversed this increased expression. Two of these, inducible nitric oxide synthase (iNOS) and phospholipase A2 (PLA2), were clearly linked to the pro-inflammatory function of activated microglia. Furthermore, we found 12 proteins, mostly enzyme proteins, which were downregulated by LPS and this was reversed by the addition of DMT. One such protein was the lysosomal 5'-3' exonuclease PLD3, which has been associated with inflammatory responses.

3.3 Suppression of autophagy in the presence of Baf

The regulation of autophagy is of crucial importance in microglial functions, and is achieved through the 62 kDa ubiquitin-binding protein/autophagosome cargo protein sequestosome 1 (p62/SQSTM1), whose level is generally inversely proportional to autophagy.

There was no statistically significant difference in microglial cell numbers in response to LPS treatment. However, the administration of Baf pretreatment led to a significant reduction in microglial proliferation, with a range of 45-50% ($p < 0.05$) observed in all treatment groups in comparison to cultures lacking Baf pretreatment. Furthermore, there was no difference between the control and LPS groups pretreated with bafilomycin (Fig. 3.12B).

Western blot showed that LPS treatment resulted in a small increase in p62 protein. Bafilomycin pretreatment did not change the amount of p62 protein. This leads us to conclude that the soluble component of the p62/SQSTM1 pool exhibited reduced sensitivity to treatments (Fig. 3.12C).

The impact of diverse inflammatory states on the distribution of p62/SQSTM1 immunoreactivity was examined in representative multicolour fluorescent immunocytochemical images (Fig. 3.12A) of control and LPS-treated microglia cultures in the absence or presence of Baf. Microglial cells that were identified by their Iba1 immunopositivity demonstrated p62/SQSTM1 immunoreactivity, both in the cytosol and compartmentalised in autophagosomes (Fig. 3.12D). The distribution of p62/SQSTM1 immunoreactivity was found to be uniform throughout the cytoplasm. In contrast, p62/SQSTM1-labelled autophagosomes were predominantly localised as puncta in the perinuclear cytoplasm and were rarely observed in the microglial processes. We found similar number of p62/SQSTM1-labeled autophagosomes in cultures challenged with LPS and in the absence or presence of Baf (Fig. 3.12D).

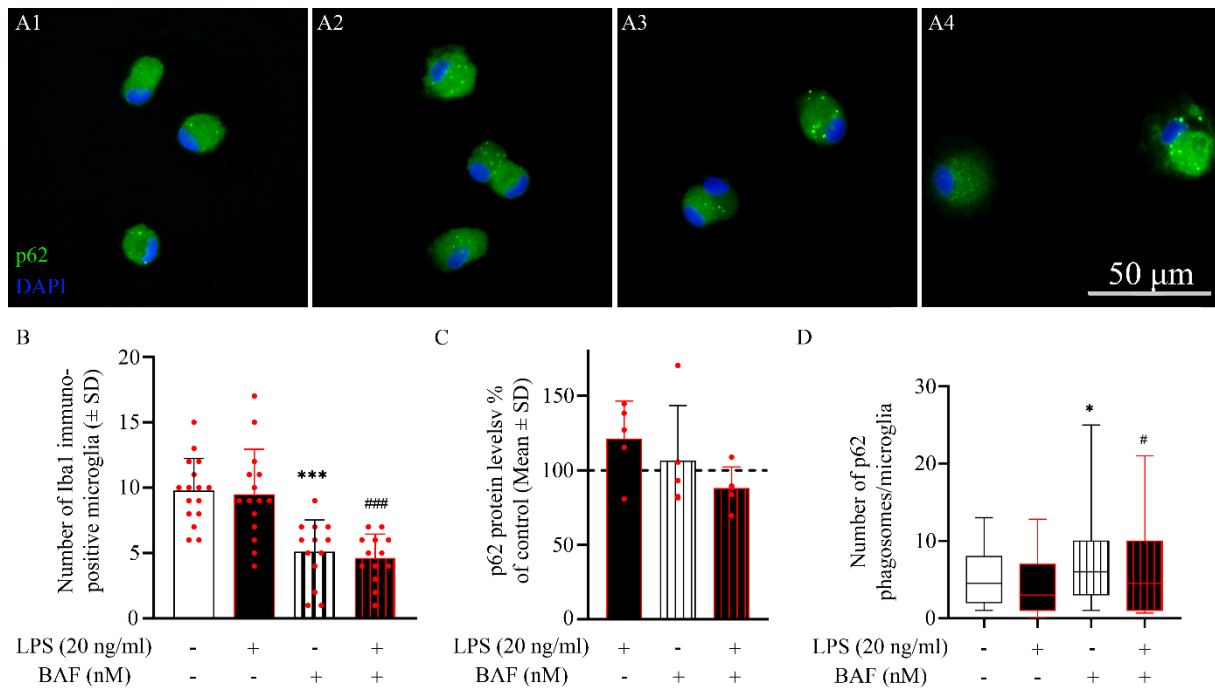


Figure 3.12 Investigation of autophagy in microglia cultures under different treatments. **A:** Representative fluorescent immunocytochemical images of microglia containing p62-immunolabeled autophagosomes. (A1) Control (unchallenged and untreated), (A2) 167 LPS-challenged, (A3) Baf pretreated + control (unchallenged and untreated), (A4) Baf pretreated + LPS-challenged microglial cells were analysed. The p62 protein was detected by incubating first with mouse anti-p62/SQSTM1 primary antibody followed by goat anti-mouse secondary antibody conjugated to Alexa Fluor 488 fluorochrome (green), while microglia nuclei are labeled with DAPI (blue). The cytoplasm of the microglia contains several p62 labeled puncta. Scale bar in A4 (for all pictures): 50 μm . **B:** The number of Iba1-positive microglial cells in control, LPS-activated cultures with or without Baf pretreatment was counted and averaged (mean (\pm SD)) The normality of the data distribution was determined using a Shapiro–Wilk test ($p < 0.001$). Data were analyzed using one-way analysis of variance (ANOVA) ($F = 15.16$, $p < 0.001$ ***), followed by Tukey’s multiple comparison. ($p < 0.001$ *** vs. absolute control; $p < 0.001$ ### vs. LPS alone). **C:** Quantitative western blot analysis of p62 immunoreactivities in secondary microglial cell cultures normalized for GAPDH immunoreactivity. The error bars indicate the integrated optical density values as % of controls (mean \pm SD of at least 4 separate experiments). The normality of the data distribution was determined using a Shapiro–Wilk test ($p = 0.419$). Data were analysed using ANOVA ($F = 1.74$, $p = 0.19$), followed by Tukey’s multiple comparison. **D:** The number of p62 immunopositive phagosomes per Iba1-positive microglia was analysed in control (unchallenged), LPS activated cultures with or without Baf pretreatment. Data are presented as 10 percentile to 90 percentile. The normality of the data distribution was determined using a Shapiro–Wilk test ($p < 0.001$). Data were analysed using a Kruskal-Wallis test ($p < 0.001$), followed by Dunn’s multiple comparison. ($p < 0.05$ * vs. absolute control; $p < 0.05$ ## vs LPS alone).

4. Discussion

4.1 Primary microglia cultures are suitable to study the pharmacological modulation of microglial activation

A complex quantitative investigation was conducted to analyse the morphological, functional and gene expression characteristics of microglia co- and monocultures from rat pups on postnatal day 1–3 following treatment with nimodipine or DMT in unstimulated or LPS-activated cultures.

Activated microglial cultures are instrumental in the testing of drugs that target neuroinflammation, as they facilitate the evaluation of drug effects on microglia without the interference of other brain cells (Sebastian-Valverde et al., 2021). These cultures enable the observation of microglia as either inactive or active based on their morphology (Szabo and Gulya, 2013; Kata et al., 2017). Phenotypic characterization captures immunostained cell morphology, indicating inactivated or activated states. Several algorithms calculate ramification index, derived from Scholl analysis or cell perimeter to surface area ratio (Faulkner et al., 2011; Szabo and Gulya, 2013; Maguire et al., 2022). Furthermore, various functional aspects, including phagocytosis, autophagy, gene and protein expression profile can be assessed. Microglia migration is assessed using specific assays, such as the transwell migration assay using chemoattractants (Rumianek and Greaves, 2020). Endocytotic and phagocytotic activity can be determined by adding specific fluorescent cargoes to the culture medium and detecting their internalization by microglia (Kata et al., 2016; Maguire et al., 2022). Microglial metabolism is a target for regulating microglial activity, as assessed by measuring oxygen consumption and extracellular acidification rates using a Seahorse Extracellular Flux Analyzer (Montilla et al., 2020). Microglial states can be identified through protein detection or gene expression profiling. Proteins, such as cytokines, can be quantified from culture media using single-protein ELISA or multiplex ELISA (Maguire et al., 2022). Mass spectrometry is used for a comprehensive analysis of protein content (Santiago et al., 2023). Proteins in the cell membrane, organelles, and cytosol can be measured using Western blot (Lam et al., 2017) or mass spectrometry (Flowers et al., 2017). Quantitative polymerase chain reaction and single-cell RNA sequencing are used for gene expression profiles (Dumas et al., 2021). Upon activation, microglia exhibit dual capacity for pro- and anti-inflammatory responses, exhibiting a continuum of polarization towards either a neurotoxic (M1) or a beneficial (M2) state in response to injury (Xiong et al., 2016). In microglial culture, M1-M2 polarization can be distinguished by examining the expression of marker proteins. The characteristic biomarkers of M1 microglia are CD86, iNOS (inducible nitric oxide synthase) and TNF- α (tumour necrosis factor alpha) (Colonna and Butovsky, 2017), while the characteristic markers of M2 microglia are CD206 (mannose receptor), Arginase-1 and IL-10 (interleukin-10) (Zhang Y. et al., 2018). Immunohistochemical staining helps to identify antigens at the tissue level. Western blot analysis of protein expression levels also provides a way to distinguish between M1 and M2 phenotypes. ELISA for quantitative detection of protein levels. Using RT-qPCR (Reverse transcription quantitative PCR), gene expression analyses can distinguish between M1 and M2 microglia, which activate different inflammation-related genes and signalling pathways (Cosma

et al., 2021). Quantitative and qualitative analysis of cytokines secreted by cells using ELISA or cytokine array techniques to determine M1 or M2 polarisation (Maguire et al., 2022). Flow cytometry is another powerful method that allows phenotypic discrimination of M1 and M2 microglia based on markers expressed on the membrane and intracellularly. Specific markers (such as CD11b, CD45) and inflammation signalling molecules (such as iNOS or Arginase-1) can be measured in the cells (Bohlen et al., 2019; Pan and Wan, 2020). Metabolic characterization M1 polarization is characterized by glycolysis, whereas M2 polarized cells rely more on oxidative phosphorylation. These metabolic pathways can be investigated by various molecular assays (e.g. Seahorse Analyzer) (Montilla et al., 2020).

The results of this investigation highlighted the complex beneficial effects of both drugs, thus classifying them as excellent candidates for preventive neuroinflammatory therapy, with well-balanced properties of enhanced anti-inflammatory and subdued proinflammatory effects.

4.2 Microglial activation is characterized by changes in calcium homeostasis, which serve as a target to attenuate neuroinflammation

As introduced above, the intracellular Ca^{2+} concentration in microglia regulates the transition from a quiescent to an activated immune effector state. In resting microglia, Ca^{2+} is present at a low concentration, whereas during activation, intracellular Ca^{2+} concentration increases rapidly (Eichhoff et al., 2011; Saddala et al., 2020). In our experiments, we targeted microglial Ca^{2+} homeostasis from two angles. First, we manipulated Ca^{2+} influx across the plasmalemma by antagonizing LVGCCs with nimodipine. Second, we pharmacologically activated intracellular Sig-1Rs with DMT. Sig-1Rs regulate Ca^{2+} transport between the MAM and mitochondria and support mitochondrial ATP production (Fig. 4.1). Both approaches suppressed microglial activation detected at the level of morphological and functional phenotypes, by modulating gene expression or protein translation.

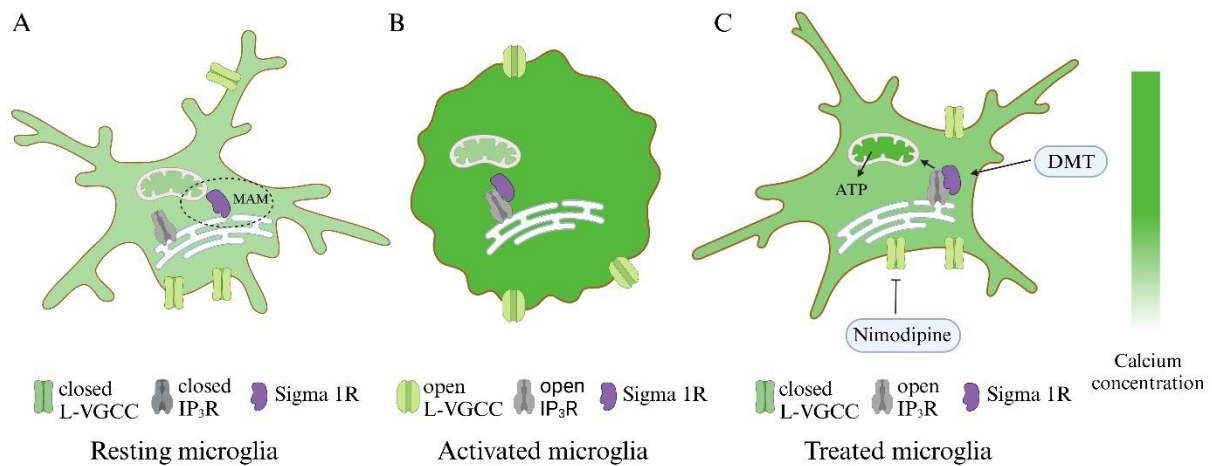


Figure 4.1 Schematic illustration of microglial calcium homeostasis and pharmacological targets. Intracellular calcium levels are low in resting microglia (A). Activation leads to an increase in intracellular calcium levels (B). Ca^{2+} influx through L-VGCCs and Ca^{2+} release from the ER via IP₃Rs are thought to contribute to the increase in intracellular Ca^{2+} concentration. Nimodipine inhibits Ca^{2+} influx through LVGCCs (C). Sigma-1 receptor is situated within the ER membrane, specifically at the mitochondria-associated ER membrane (MAM) (A). DMT targets sigma-1 receptors to stabilize IP₃R to maintain Ca^{2+} flow from the ER to mitochondria to support ATP production (C). Light green indicates low calcium levels, while dark green indicates high calcium levels (scale to the right).

4.2.1 Benefits of nimodipine application for neuroinflammation

There is a prevailing consensus that the activation of microglia is linked to an increase in the intracellular concentration of Ca^{2+} when exposed to a range of danger signals (Hopp et al., 2020), with LPS being one of the most commonly used activators (Hoffmann et al., 2003). Here, we treated LPS-activated microglia with nimodipine, an LVGCC blocker, to investigate whether manipulation of microglial Ca^{2+} homeostasis via LVGCC antagonism inhibits microglial activation.

In addition to confirming that LPS exposure causes a shift in microglial morphological and functional phenotype, we have identified a complex interplay of Ca^{2+} ion channel expression during microglial activation. Here, we show that LPS upregulates the expression of purinergic P2X4 receptors and TRPM2 channels, suggesting that Ca^{2+} accumulation during microglial activation may be manifested through these pathways. These data of ours are consistent with the upregulation of P2X4 receptors in neuroinflammatory states of the brain and spinal cord (Montilla et al., 2020), and the involvement of TRPM2 channels in the promotion of microglial inflammatory polarization (Raghunatha et al., 2020).

Along with the upregulation of P2X4 receptors and TRPM2 channels, the expression of ryanodine and IP3 receptor genes and SERCA pump genes (Atp2a2 and Atp2a3) at the endoplasmic reticulum (ER) were altered in a compensatory manner. Ryanodine and IP3 receptors, which release Ca^{2+} from the ER into the cytoplasm, were downregulated, whereas

SERCA, which pumps Ca^{2+} from the cytoplasm into the ER lumen, was upregulated. These changes suggest that the Ca^{2+} concentration, which presumably increases via P2X4 receptors and TRPM2 channels upon microglial activation, is counterbalanced by mechanisms at the ER.

Nimodipine consistently inhibited the phenotypic shift of microglia in co-cultures and monocultures, suggesting that microglia were reliably targeted by the treatment. In addition, we previously demonstrated that nimodipine suppressed microglial activation in live brain slice preparations challenged by metabolic stress (Frank et al., 2024). Driven by these data, we explored DEGs underlying these microglial morphological and functional phenotypic changes. Based on our findings, we suggest that nimodipine finely modulates intracellular signaling pathways (e.g., expression of protein kinases) by inhibiting LVGCC to induce the gene expression changes. Because Ca^{2+} is a well-known intracellular second messenger involved in the control of gene expression, we suggest that nimodipine achieved its anti-inflammatory effect by the modulation of intracellular Ca^{2+} signaling (Barbado et al., 2009). Indeed, Barbado et al. (2009) reviewed three Ca^{2+} -dependent gene transcriptional pathways regulated by VGCCs. These pathways include a calmodulin-dependent kinase and cAMP response element binding protein (CREB)-dependent pathway, a signal transduction pathway initiated by Ca^{2+} -sensitive proteins that are associated with the VGCC signaling complex, and a pathway regulated by Ca^{2+} -binding transcription factors (e.g., DREAM). Finally, the intracellular carboxyl terminus of the α subunit of LVGCCs contains a proteolytic fragment. This fragment has been identified to act as a transcription factor by its translocation to the cell nucleus (Gomez-Ospina et al., 2006; Lu et al., 2015).

Although in our hands nimodipine was applied according to its widely accepted action as an agent to block LVGCCs, Ca^{2+} channel blockers belonging to the class of dihydropyridines may target alternative cellular sites. These alternative targets are Kv1.3 voltage-gated potassium channels (Kazama et al., 2013), mineralocorticoid receptors (Dietz, Du et al., 2008), and CFTR chloride channels (Pedemonte et al., 2005), raising the possibility that suppressed activation of these pathways contributes to the effect of nimodipine seen here.

In conclusion, in addition to the approved use of nimodipine to achieve cerebral vasodilation in aneurysmal subarachnoid hemorrhage, our data point in the direction of expanding the medical field of indication of nimodipine to attenuate neuroinflammation in acute brain injury or chronic neurodegeneration.

4.2.2 The therapeutic potential of DMT for neuroinflammation

DMT is a fascinating compound in its own right, not only for its psychedelic properties but also for its noteworthy neuroprotective effects and potential therapeutic applications (Carbonaro and Gatch, 2016). It plays a critical role in the central nervous system, especially under conditions of stress, by protecting neurons, reducing inflammation, and promoting neuroplasticity through mechanisms such as the elevation of brain-derived neurotrophic factor (BDNF) (de Almeida et al., 2019). Sig-1Rs are intracellular receptors that localize to a specific region of the endoplasmic reticulum (ER) membrane that is connected to the outer mitochondrial membrane (mitochondria-associated ER membrane, MAM). These receptors have been shown to regulate Ca^{2+} balance within cells, inhibit ROS production, and promote cell survival in conditions of stress (Hayashi, 2015; Penke et al., 2018). A substantial body of experimental evidence indicates that Sig-1R activation exerts neuroprotective effects in the context of ischemic stroke.

In experimental cerebral ischemia, DMT has been shown to be neuroprotective (Szabó et al., 2021), reducing brain infarct size, improving motor function and inhibiting the transcription of mRNA for pro-inflammatory cytokines in the brain (Nardai et al., 2020). In previous studies, researchers attributed the beneficial effects of DMT to Sig-1R activation. In vivo studies have also demonstrated that, in addition to neurons, microglia also express the target of DMT, Sig-1R (Nardai et al., 2020; Szabó et al., 2021). However, in the intact brain, the effect of DMT is complex, and the effect on microglia is difficult to isolate.

In our microglia cultures, the administration of DMT has been demonstrated to induce alterations in microglial morphology and functionality. DMT when added to activated microglia cultures at concentrations of 20 and 50 μM resulted in more ramified cell shapes. Also, at the same concentrations, DMT reduced the proportion of phagocytosing cells in the culture, as visualized by fluorescent synthetic polymer microbeads. Taken together, these results suggest that DMT reduces microglial activation. Furthermore, proteomic analysis here has revealed substantial changes in the concentrations of proteins, with DMT reversing the expression of specific pro-inflammatory proteins that have been previously induced by LPS.

The inhibition of microglial activation observed here is consistent with previous findings that DMT was protective in macrophage cultures of monocyte origin exposed to hypoxia (Szabo et al., 2016). Agonism of Sig-1R, the target of DMT with other synthetic agents (SKF10047) also inhibited microglial activation and M1 polarization (Ooi et al., 2021). In cultures exposed to microglia-damaging levels of hypoxia, agonism of Sig-1R with pentazocine prevented

microglial death (Heiss et al., 2016). Thus, agonism of Sig-1R with DMT may be protective for microglial cells under lethal conditions. In the presence of a stimulus that induces microglial activation as demonstrated by the present experiments, DMT appears to inhibit microglial activation. Finally, in a rodent model of focal cerebral ischemia, DMT inhibited the mRNA transcription of pro-inflammatory cytokines, including TNF- α , and thus an anti-neuroinflammatory effect was reported (Nardai et al., 2020). Our results suggest that the protective effect of DMT against neuroinflammation in experimental stroke may have been exerted directly on microglial cells by inhibiting microglial activation.

DMT alone did not affect phagocytosis, but reduced the proportion of phagocytosing cells in LPS-activated microglia. There is no prior experimental evidence to support that Sig-1R agonism should limit microglial phagocytosis, but the transfer of Sig-1R intact macrophages to recipient Sig-1R knockout mice highlighted the essential role of Sig-1R in phagocytosis (Zhang et al., 2023).

The shift from 111 upregulated proteins in the presence of LPS to just 21 with co-administration of DMT suggests a regulatory role for DMT in protein expression dynamics. This suggests that DMT mitigates the inflammatory response possibly by the downregulation of certain proteins. Among the proteins whose expression is increased by LPS and then inhibited by DMT, we identified inducible nitric oxide synthase (iNOS) and phospholipase A2 (PLA2). iNOS catalyzes the production of the bioactive free radical nitric oxide (NO). In vivo, microglia do not express iNOS, but under inflammatory conditions, activated microglia in mice, rats and humans express iNOS as part of their response to inflammation and injury (Galea et al., 1992). As with iNOS, upregulation of PLA2 is a hallmark of inflammatory conditions. PLA2 catalyzes the release of arachidonic acid, which is then utilized in the production of inflammatory lipid mediators, such as prostanoids. This process is of crucial importance in various inflammatory processes. Pharmacological inhibition of PLA2 in microglial cells has been shown to prevent ROS production and secretion of pro-inflammatory cytokines (Yang et al., 2009).

In addition, the exonuclease phospholipase D family member 3 (PLD3) was identified among the proteins whose downregulation by LPS was counteracted by DMT. PLD3 5'-3' exonuclease, a lysosomal nucleic acid degradation enzyme, has been implicated in autoimmune inflammatory diseases. PLD3 has been shown to inhibit autoimmune inflammatory responses by cleaving nucleic acids (Gavin et al., 2021). In the context of our microglial cultures, the presence of LPS resulted in a decrease in PLD3 protein levels. However, the subsequent addition of DMT resulted in an increase in PLD3 protein levels, suggesting an enhanced anti-inflammatory action. From the observations made here, it is clear that DMT treatment in

inflammatory processes exerts an anti-microglial activation effect reflected by the modulation of the levels of the proteins involved.

In conclusion, morphological and functional characterization of microglial activation and proteomic analysis showed that DMT inhibited microglial activation in LPS-activated primary microglial cultures. These observations may be useful in the development of drugs for the treatment of diseases in which neuroinflammation impairs the chances of recovery. DMT has also recently attracted the attention of pharmaceutical companies, with Canada's Algernon Pharmaceuticals (<https://www.algernonpharmaceuticals.com/about>) testing DMT in the treatment of stroke (<https://www.algernonpharmaceuticals.com/pipeline/ap-188-dmt>), and the use of DMT is currently being evaluated in Phase 1 clinical trials. Our experimental results thus have clinical potential and will contribute to a better understanding of the mechanism of action of DMT.

4.3 The suppression of microglial autophagy is coincident with an increase in p62/SQSTM1 protein

The present study investigates the role of autophagy regulation in microglial functions, with a particular focus on the protein p62/SQSTM1. The results demonstrate that while LPS treatment did not result in a significant alteration of microglial cell numbers, pretreatment with Baf led to a substantial reduction in microglial proliferation, with a decrease of 45-50%.

Autophagy and microglial cells are integral to maintaining cellular homeostasis and responding to various stressors in the central nervous system. (Peng et al., 2022). Autophagy facilitates the degradation and recycling of damaged cellular components, particularly under pathological conditions like ischemia and hypoxia, while also influencing neuroinflammation through the polarization of microglial cells. (Parzych and Klionsky, 2014; Lian et al., 2021). In mammals, autophagy frequently converges with the endocytic pathway, whereby the process of formation of autolysosomes occurs, resulting from the fusion of the two other types of vesicle, namely the autophagosome and the lysosome. The final outcome of this process is the degradation of cytoplasmic cargoes by hydrolases (Klionsky, 2007). It is evident that autophagy and inflammatory processes are closely linked, with critical regulatory molecules such as p62/SQSTM1 playing pivotal roles. Inhibition of autophagy has been observed to result in increased p62/SQSTM1 levels, while its activation has been shown to lead to reduced protein levels. p62/SQSTM1 plays a crucial role in the proteasomal degradation process and the regulation of protein aggregates (Ye et al., 2020). Consequently, variations in p62/SQSTM1

levels can serve as a marker for monitoring autophagy flux, underscoring its significance in the dynamic interplay of these biological processes (Pesti et al., 2024).

The present study highlights the intricate role of p62/SQSTM1 in regulating autophagy within microglial functions, particularly under inflammatory conditions induced by LPS. While the absence of significant changes in microglial cell numbers suggests that LPS treatment does not directly influence proliferation, the notable reduction in microglial proliferation upon bafilomycin pretreatment underscores the complex interactions between autophagy and inflammation. The observed effect on proliferation is likely attributable to the inhibition of autophagy, which is known to be dependent upon the inhibition of vacuolar ATPase (V-ATPase) (Lu et al., 2015). Bafilomycin is well known to possess both cytostatic and apoptotic properties (Xie et al., 2014) but, to the best of our knowledge, this is the first occasion on which an effect of this kind on microglia proliferation has been reported. The observed increase in p62 protein levels in response to LPS, alongside its stable concentration with bafilomycin pretreatment, suggests a nuanced role of p62 in inflammatory states that warrants further investigation. The uniform presence of p62/SQSTM1 across the cytoplasm highlights its fundamental role in microglial function, while the concentrated perinuclear localization of autophagosomes signifies a nuanced response to inflammatory stimuli. The slight decrease observed in the number of autophagosomes after LPS treatment compared to the control group is analogous to that seen in BV2 cells (He et al., 2017), although this change did not reach statistical significance, in contrast to the group that had been pre-treated with bafilomycin. The results obtained in this study corroborate earlier research findings regarding the impact of bafilomycin on the regulation of autophagy. Furthermore, the present study provides additional evidence to support the role of bafilomycin in modulating autophagic processes, highlighting its potential effects on cellular responses and autophagy-related pathways.

Moreover, the interplay between ion homeostasis and signaling pathways, notably through TLR4 and VGCCs, underscores microglia cells regulatory roles in inflammatory responses post-injury. Ultimately, understanding the nuanced behavior of microglia and their modulation represents a promising therapeutic avenue for addressing central nervous system disorders, particularly in optimizing responses following ischemic strokes (Cojocaru et al., 2021; Jin et al., 2019).

5. Main observations and conclusions

This study explores the pharmacological modulation of microglia and highlights potential therapeutic strategies to suppress their activation in neuroinflammatory conditions. Three key interventions were investigated: nimodipine, dimethyltryptamine (DMT), and LPS-induced autophagy inhibition.

1. The study demonstrated that nimodipine, a selective blocker of L-type voltage-gated calcium channels (LVGCCs), attenuates microglial activation. Through morphological and functional profiling, as well as transcriptomic analysis, the data revealed that nimodipine suppresses microglial activation by modulating intracellular Ca^{2+} signaling. LPS exposure typically triggers microglial activation, accompanied by an increase in intracellular Ca^{2+} , which is hypothesized to occur through P2X4 receptors and TRPM2 channels. However, nimodipine's action on LVGCCs reduces calcium influx, leading to altered gene expression and a dampened inflammatory response. This modulation of calcium signaling provides a mechanism for nimodipine's anti-inflammatory effect, suggesting its potential for mitigating neuroinflammation in acute brain injury or chronic neurodegenerative diseases.
2. The study also explored the effects of DMT on microglial activation. DMT administration resulted in significant changes in microglial morphology, shifting them towards more ramified shapes and reducing their phagocytic activity, which indicates a decrease in microglial activation. Proteomic analysis further revealed that DMT reversed the upregulation of pro-inflammatory proteins induced by LPS, such as inducible nitric oxide synthase (iNOS) and phospholipase A2 (PLA2). This shift in protein expression, from 111 upregulated proteins with LPS to only 21 with DMT, suggests that DMT exerts anti-inflammatory effects, possibly through its action on the Sig-1R receptor, a known intracellular target. The reduction in pro-inflammatory protein expression reinforces DMT's potential to regulate microglial activation in inflammatory conditions.
3. The study further examined the relationship between autophagy and inflammation in microglia. LPS exposure, when combined with Bafilomycin A1 (Baf) pretreatment, inhibited microglial autophagic activity, evidenced by increased levels of p62/SQSTM1 protein. This suggests a disruption in autophagy that could contribute to sustained inflammation. The findings underscore the importance of autophagy in regulating microglial function and inflammation, and highlight the complex interplay between ion

homeostasis, signaling pathways, and autophagic activity in microglial responses post-injury.

In conclusion, the study demonstrates that nimodipine and DMT can modulate microglial activation through distinct cellular mechanisms, offering potential therapeutic strategies for managing neuroinflammatory diseases. Additionally, the interplay between autophagy and inflammation provides further insights into how microglia can be targeted for therapeutic benefit in central nervous system disorders.

6. Summary

Background: Microglia exhibit elevated intracellular Ca^{2+} concentrations in response to acute brain injury. In turn, intracellular Ca^{2+} transients have been postulated to regulate microglial activation which initiates neuroinflammation and pro-inflammatory cytokine production. Microglia are endowed with L-type voltage-gated Ca^{2+} channels (LVGCCs), which have been implicated in microglial Ca^{2+} accumulation. Microglia also express sigma-1 receptors (Sig-1R) on the mitochondria-associated membranes (MAM) of the endoplasmic reticulum (ER), which have been implicated in the cellular stress response.

Here, we tested whether pharmacological inhibition of L-type voltage-gated Ca^{2+} channels with nimodipine suppresses the shift of microglia from a quiescent to an activated phenotype and how it modulates microglial gene expression. We also tested whether pharmacological activation of Sig-1R with *N,N*-dimethyltryptamine (DMT) suppresses the shift of microglia from a quiescent to an activated phenotype and how it modulates microglial proteomics.

Autophagy also impacts microglia function, with TLR4 acting as an upstream regulator. Lipopolysaccharide can activate the PI3K/AKT/mTOR pathway in microglia, inhibiting autophagic flow and enhancing the inflammatory response. We tested whether Bafilomycin A1 can block this process.

Methods: Primary microglial cultures were prepared from the cortex of neonatal Sprague-Dawley rats. On day 6, the plated cells were activated with lipopolysaccharide (LPS; 20 ng/ml) to activate microglia. In the first set of experiments, cultures were treated with nimodipine alone (5-10-20 μM) or in combination with LPS for 24 h. In the second set of experiments, cultures were treated with DMT (Sig-1R agonist) alone (5-10-20-50 μM) or in combination with LPS for 24 h. In the third set of experiments, microglial cultures were pre-treated with Baf A1 (50nM) for 3h, and activated with LPS for 24h. Microglial activation was evaluated by Iba1 immunolabeling. The degree of arborization was expressed by a transformation index (TI)

calculated from the cell perimeter and surface area. Iba1 protein levels were quantified by Western blot analysis, and the phagocytic activity was visualized with fluorescent microbeads. TNF- α cytokine levels in the cell culture medium were measured with ELISA. Total RNA was isolated from collected cells and processed for RNA sequencing (RNA-seq) to determine differentially expressed genes (DEGs). Proteins were isolated from harvested cells and processed for proteomic analysis with mass spectrometry.

Results: When the LPS-challenged cell cultures were treated with nimodipine, significantly more ramified cells were seen at the 10 μ M and 20 μ M concentrations. Increased Iba1 signal intensity in Western blot analysis confirmed microglial activation due to LPS treatment, which was decreased particularly by 10 and 20 μ M nimodipine. Control microglia engulfed a few microbeads. In contrast, LPS challenge increased microglial phagocytic activity, which was significantly attenuated by nimodipine. Nimodipine produced a stepwise reduction in TNF- α levels along its increasing concentration, although without statistical significance. The RNA-seq data here identified the expression of the *Cacna1c* and the *Cacna1d* genes in primary microglia cultures, which encode Cav1.2 and Cav1.3 subtypes of the α 1 subunit of LVGCCs. As expected, LPS treatment resulted in robust transcriptomic changes in rat microglia affecting 3554 genes including proteins of the TLR4 intracellular signaling cascade, chemokines and interleukins. Nimodipine treatment of LPS-activated microglia altered the expression of 110 genes compared to LPS treatment alone.

When the LPS-treated cell cultures were treated with DMT, significantly more ramified cells were observed. Increased Iba1 signal intensity in Western blot analysis confirmed microglial activation by LPS treatment, which was also increased by DMT. LPS challenge increased microglial phagocytic activity, which was significantly attenuated by DMT. The proteomics data identified a total of 2793 proteins, of which 244 were altered in abundance. The combined administration of DMT and LPS resulted in the upregulation of 21 proteins and the downregulation of 84 proteins compared to LPS given alone. Importantly, DMT treatment counteracted the LPS-induced synthesis of proteins implicated in pro-inflammatory signaling (e.g. iNOS and PLA2).

In the regulation of autophagy, LPS treatment did not significantly affect microglial cell numbers, but Baf pretreatment reduced microglial proliferation. LPS treatment resulted in a small increase in p62 protein, but bafilomycin pretreatment did not change the amount. p62/SQSTM1 immunoreactivity was uniform throughout the cytoplasm, with autophagosomes predominantly localized in the perinuclear cytoplasm.

Conclusions: Nimodipine is used to alleviate delayed ischemic deficit after aneurismal subarachnoid hemorrhage. Our data suggest that nimodipine may also be applicable to attenuate microglial activation. Nimodipine appears to exert its anti-inflammatory effects by modulating microglial Ca^{2+} homeostasis. In conclusion, the effect of nimodipine goes beyond cerebral vasorelaxation and its anti-inflammatory potential may be considered in cerebral ischemia, where progressive neuronal injury is thought to be associated with neurotoxic microglial activation.

DMT promoted the quiescent state of microglia compared to LPS. We hypothesize that DMT exerts its effect by modifying the ER stress response and microglial Ca^{2+} homeostasis. This hypothesis is supported by previous findings that microglial activation is associated with increased intracellular Ca^{2+} concentration and that Sig-1R in the MAM regulates Ca^{2+} transport between the ER and mitochondria.

LPS treatments suppressed autophagic activity, leading to an increase in p62/SQSTM1 protein. Pretreatment with BAF improved regulatory effects, revealing the complexity of autophagy regulation in inflammation and microglial cell modulation.

7. Funding

This work was supported by the EU's Horizon 2020 research and innovation program grant number 739593; the National Research, Development and Innovation Office of Hungary (grant numbers K134334, K134377, K146725); the Ministry of Innovation and Technology of Hungary and the National Research, Development and Innovation Fund (grant number TKP2021-EGA-28 financed under the TKP2021-EGA funding scheme); the National Brain Research Program 3.0 of the Hungarian Academy of Sciences; and the Research Fund of the Albert Szent-Györgyi Medical School, University of Szeged, Hungary.

This work was funded by grants from the Ministry of National Resources (GINOP 2.3.2-15-2016-00030 and 2.3.2-15-2016-00034) through the European Union Cohesion Fund and from the EU's Horizon 2020 Research and Innovation Program (grant number 739593).

8. Acknowledgements

First of all, I would like to express my sincere gratitude to Prof. Dr. Károly Gulya for giving me the opportunity to work in his research group and for believing in me.

I would like to thank the help and support of my colleagues and former colleagues in the research group: Dr. Anna Törteli, Dr. Réka Tóth, Dr. Armand Rafael Bálint, Dr. Szilvia V. Kecskés, Dr. Péter Archibald Szarvas, Dr. Rita Frank and Dr. Ákos Menyhárt. Special thanks to Dr. Diana Kata who was always there to help me.

I am grateful to my friends for supporting me, although they usually do not understand what I am talking about and what my job is seriously. Words cannot describe how grateful I am to my family for giving me inspiring thoughts in difficult times, believing in me and being very patient.

Last but not least, I would like to thank my supervisor: Prof. Dr. Eszter Farkas offered me the opportunity to join her research group as a Ph.D. student. Her enthusiasm, vision, dedication, ideas and humility towards science have been an inspiration to good scientific practice. I couldn't imagine a better supervisor.

9. References

- Agalave NM, Lane BT, Mody PH, Szabo-Pardi TA, Burton MD. Isolation, culture, and downstream characterization of primary microglia and astrocytes from adult rodent brain and spinal cord. *J Neurosci Methods*. 2020 Jul 1;340:108742. doi: 10.1016/j.jneumeth.2020.108742. Epub 2020 Apr 19. PMID: 32315669; PMCID: PMC7293863.
- Akhmetzyanova ER, Rizvanov AA, Mukhamedshina YO. Current methods for the microglia isolation: Overview and comparative analysis of approaches. *Cell Tissue Res*. 2024 Feb;395(2):147-158. doi: 10.1007/s00441-023-03853-8. Epub 2023 Dec 15. PMID: 38099956.
- Barbado M, Fablet K, Ronjat M, De Waard M. Gene regulation by voltage-dependent calcium channels. *Biochim Biophys Acta*. 2009 Jun;1793(6):1096-104. doi: 10.1016/j.bbamcr.2009.02.004. Epub 2009 Feb 27. PMID: 19250948.
- Bean BP. Neurotransmitter inhibition of neuronal calcium currents by changes in channel voltage dependence. *Nature*. 1989 Jul 13;340(6229):153-6. doi: 10.1038/340153a0. PMID: 2567963.
- Bouso JC, Andi3n 3, Sarris JJ, Scheidegger M, T3foli LF, Opaleye ES, Schubert V, Perkins D. Adverse effects of ayahuasca: Results from the Global Ayahuasca Survey. *PLOS Glob Public Health*. 2022 Nov 16;2(11):e0000438. doi: 10.1371/journal.pgph.0000438. PMID: 36962494; PMCID: PMC10021266.
- Cadiz MP, Jensen TD, Sens JP, Zhu K, Song WM, Zhang B, Ebbert M, Chang R, Fryer JD. Culture shock: microglial heterogeneity, activation, and disrupted single-cell microglial networks in vitro. *Mol Neurodegener*. 2022 Mar 28;17(1):26. doi: 10.1186/s13024-022-00531-1. PMID: 35346293; PMCID: PMC8962153.
- Carbonaro TM, Gatch MB. Neuropharmacology of N,N-dimethyltryptamine. *Brain Res Bull*. 2016 Sep;126(Pt 1):74-88. doi: 10.1016/j.brainresbull.2016.04.016. Epub 2016 Apr 25. PMID: 27126737; PMCID: PMC5048497.
- Carlson AP, H3nggi D, Macdonald RL, Shuttleworth CW. Nimodipine Reappraised: An Old Drug With a Future. *Curr Neuropharmacol*. 2020;18(1):65-82. doi: 10.2174/1570159X17666190927113021. PMID: 31560289; PMCID: PMC7327937.
- Cs3sz3r E, L3n3rt N, Cser3p C, K3rnyei Z, Fekete R, P3sfai B, Bal3zsf3 D, Hangya B, Schwarcz AD, Szabadits E, Sz3ll3si D, Szigeti K, M3th3 D, West BL, Sviatk3 K, Br3s AR, Mariani JC, Kliewer A, Lenkei Z, Hricis3k L, Beny3 Z, Baranyi M, Sperl3gh B, Menyh3rt 3,

- Farkas E, Dénes Á. Microglia modulate blood flow, neurovascular coupling, and hypoperfusion via purinergic actions. *J Exp Med*. 2022 Mar 7;219(3):e20211071. doi: 10.1084/jem.20211071. Epub 2022 Feb 24. PMID: 35201268; PMCID: PMC8932534.
- Cojocaru A, Burada E, Bălșeanu AT, Deftu AF, Cătălin B, Popa-Wagner A, Osiac E. Roles of Microglial Ion Channel in Neurodegenerative Diseases. *J Clin Med*. 2021 Mar 17;10(6):1239. doi: 10.3390/jcm10061239. PMID: 33802786; PMCID: PMC8002406.
- Colonna M, Butovsky O. Microglia Function in the Central Nervous System During Health and Neurodegeneration. *Annu Rev Immunol*. 2017 Apr 26;35:441-468. doi: 10.1146/annurev-immunol-051116-052358. Epub 2017 Feb 9. PMID: 28226226; PMCID: PMC8167938.
- Cosma NC, Üsekes B, Otto LR, Gerike S, Heuser I, Regen F, Hellmann-Regen J. M1/M2 polarization in major depressive disorder: Disentangling state from trait effects in an individualized cell-culture-based approach. *Brain Behav Immun*. 2021 May;94:185-195. doi: 10.1016/j.bbi.2021.02.009. Epub 2021 Feb 17. PMID: 33607231.
- Das JM, Zito PM. Nimodipine. 2024 May 7. In: StatPearls [Internet]. Treasure Island (FL): StatPearls Publishing; 2025 Jan-. PMID: 30521291.
- de Almeida RN, Galvão ACM, da Silva FS, Silva EADS, Palhano-Fontes F, Maia-de-Oliveira JP, de Araújo LB, Lobão-Soares B, Galvão-Coelho NL. Modulation of Serum Brain-Derived Neurotrophic Factor by a Single Dose of Ayahuasca: Observation From a Randomized Controlled Trial. *Front Psychol*. 2019 Jun 4;10:1234. doi: 10.3389/fpsyg.2019.01234. PMID: 31231276; PMCID: PMC6558429.
- Dean JG. Indolethylamine-N-methyltransferase Polymorphisms: Genetic and Biochemical Approaches for Study of Endogenous N,N,-dimethyltryptamine. *Front Neurosci*. 2018 Apr 23;12:232. doi: 10.3389/fnins.2018.00232. PMID: 29740267; PMCID: PMC5924808.
- Denaro S, Pasquinucci L, Turnaturi R, Alberghina C, Longhitano L, Giallongo S, Costanzo G, Spoto S, Grasso M, Zappalà A, Li Volti G, Tibullo D, Vicario N, Parenti R, Parenti C. Sigma-1 Receptor Inhibition Reduces Mechanical Allodynia and Modulate Neuroinflammation in Chronic Neuropathic Pain. *Mol Neurobiol*. 2024 May;61(5):2672-2685. doi: 10.1007/s12035-023-03717-w. Epub 2023 Nov 3. PMID: 37922065; PMCID: PMC11043107.
- Dietz JD, Du S, Bolten CW, Payne MA, Xia C, Blinn JR, Funder JW, Hu X. A number of marketed dihydropyridine calcium channel blockers have mineralocorticoid receptor antagonist activity. *Hypertension*. 2008 Mar;51(3):742-8. doi: 10.1161/HYPERTENSIONAHA.107.103580. Epub 2008 Feb 4. PMID: 18250364.

- Dumas AA, Borst K, Prinz M. Current tools to interrogate microglial biology. *Neuron*. 2021 Sep 15;109(18):2805-2819. doi: 10.1016/j.neuron.2021.07.004. Epub 2021 Aug 13. PMID: 34390649.
- Egger K, Gudmundsen F, Jessen NS, Baun C, Poetzsch SN, Shalgunov V, Herth MM, Quednow BB, Martin-Soelch C, Dornbierer D, Scheidegger M, Cumming P, Palner M. A pilot study of cerebral metabolism and serotonin 5-HT_{2A} receptor occupancy in rats treated with the psychedelic tryptamine DMT in conjunction with the MAO inhibitor harmine. *Front Pharmacol*. 2023 Sep 28;14:1140656. doi: 10.3389/fphar.2023.1140656. PMID: 37841918; PMCID: PMC10568461.
- Eichhoff G, Brawek B, Garaschuk O. Microglial calcium signal acts as a rapid sensor of single neuron damage in vivo. *Biochim Biophys Acta*. 2011 May;1813(5):1014-24. doi: 10.1016/j.bbamer.2010.10.018. Epub 2010 Nov 5. PMID: 21056596.
- Espinosa-Parrilla JF, Martínez-Moreno M, Gasull X, Mahy N, Rodríguez MJ. The L-type voltage-gated calcium channel modulates microglial pro-inflammatory activity. *Mol Cell Neurosci*. 2015 Jan;64:104-15. doi: 10.1016/j.mcn.2014.12.004. Epub 2014 Dec 12. PMID: 25497271.
- Faulkner S, Bainbridge A, Kato T, Chandrasekaran M, Kapetanakis AB, Hristova M, Liu M, Evans S, De Vita E, Kelen D, Sanders RD, Edwards AD, Maze M, Cady EB, Raivich G, Robertson NJ. Xenon augmented hypothermia reduces early lactate/N-acetylaspartate and cell death in perinatal asphyxia. *Ann Neurol*. 2011 Jul;70(1):133-50. doi: 10.1002/ana.22387. Epub 2011 Jun 14. PMID: 21674582.
- Feng Y, Hu X, Zhang Y, Wang Y. The Role of Microglia in Brain Metastases: Mechanisms and Strategies. *Aging Dis*. 2024 Feb 1;15(1):169-185. doi: 10.14336/AD.2023.0514. PMID: 37307835; PMCID: PMC10796095.
- Feng Y, Wang B, Du F, Li H, Wang S, Hu C, Zhu C, Yu X. The involvement of PI3K-mediated and L-VGCC-gated transient Ca²⁺ influx in 17β-estradiol-mediated protection of retinal cells from H₂O₂-induced apoptosis with Ca²⁺ overload. *PLoS One*. 2013 Nov 5;8(11):e77218. doi: 10.1371/journal.pone.0077218. PMID: 24223708; PMCID: PMC3818527.
- Flowers A, Bell-Temin H, Jalloh A, Stevens SM Jr, Bickford PC. Proteomic analysis of aged microglia: shifts in transcription, bioenergetics, and nutrient response. *J Neuroinflammation*. 2017 May 3;14(1):96. doi: 10.1186/s12974-017-0840-7. PMID: 28468668; PMCID: PMC5415769.

- Frank R, Szarvas PA, Pesti I, Zsigmond A, Berkecz R, Menyhárt Á, Bari F, Farkas E. Nimodipine inhibits spreading depolarization, ischemic injury, and neuroinflammation in mouse live brain slice preparations. *Eur J Pharmacol.* 2024 Aug 15;977:176718. doi: 10.1016/j.ejphar.2024.176718. Epub 2024 Jun 6. PMID: 38849040.
- Fu R, Shen Q, Xu P, Luo JJ, Tang Y. Phagocytosis of microglia in the central nervous system diseases. *Mol Neurobiol.* 2014 Jun;49(3):1422-34. doi: 10.1007/s12035-013-8620-6. Epub 2014 Jan 7. PMID: 24395130; PMCID: PMC4012154.
- Fujita H, Tanaka J, Toku K, Tateishi N, Suzuki Y, Matsuda S, Sakanaka M, Maeda N. Effects of GM-CSF and ordinary supplements on the ramification of microglia in culture: a morphometrical study. *Glia.* 1996 Dec;18(4):269-81. doi: 10.1002/(sici)1098-1136(199612)18:4<269::aid-glia2>3.0.co;2-t. PMID: 8972796.
- Galea E, Feinstein DL, Reis DJ. Induction of calcium-independent nitric oxide synthase activity in primary rat glial cultures. *Proc Natl Acad Sci U S A.* 1992 Nov 15;89(22):10945-9. doi: 10.1073/pnas.89.22.10945. PMID: 1279698; PMCID: PMC50459.
- Gavin AL, Huang D, Blane TR, Thinnes TC, Murakami Y, Fukui R, Miyake K, Nemazee D. Cleavage of DNA and RNA by PLD3 and PLD4 limits autoinflammatory triggering by multiple sensors. *Nat Commun.* 2021 Oct 7;12(1):5874. doi: 10.1038/s41467-021-26150-w. PMID: 34620855; PMCID: PMC8497607.
- Gomez-Ospina N, Tsuruta F, Barreto-Chang O, Hu L, Dolmetsch R. The C terminus of the L-type voltage-gated calcium channel Ca(V)1.2 encodes a transcription factor. *Cell.* 2006 Nov 3;127(3):591-606. doi: 10.1016/j.cell.2006.10.017. PMID: 17081980; PMCID: PMC1750862.
- Gruol DL, Vo K, Bray JG. Increased astrocyte expression of IL-6 or CCL2 in transgenic mice alters levels of hippocampal and cerebellar proteins. *Front Cell Neurosci.* 2014 Aug 14;8:234. doi: 10.3389/fncel.2014.00234. PMID: 25177271; PMCID: PMC4132577.
- Hall AA, Herrera Y, Ajmo CT Jr, Cuevas J, Pennypacker KR. Sigma receptors suppress multiple aspects of microglial activation. *Glia.* 2009 May;57(7):744-54. doi: 10.1002/glia.20802. PMID: 19031439; PMCID: PMC2692292.
- Hamilton SP, Rome LH. Stimulation of in vitro myelin synthesis by microglia. *Glia.* 1994 Aug;11(4):326-35. doi: 10.1002/glia.440110405. PMID: 7960036.
- Han HE, Kim TK, Son HJ, Park WJ, Han PL. Activation of Autophagy Pathway Suppresses the Expression of iNOS, IL6 and Cell Death of LPS-Stimulated Microglia Cells. *Biomol Ther (Seoul).* 2013 Jan;21(1):21-8. doi: 10.4062/biomolther.2012.089. PMID: 24009854; PMCID: PMC3762303.

- Haruwaka K, Ying Y, Liang Y, Umpierre AD, Yi MH, Kremen V, Chen T, Xie T, Qi F, Zhao S, Zheng J, Liu YU, Dong H, Worrell GA, Wu LJ. Microglia enhance post-anesthesia neuronal activity by shielding inhibitory synapses. *Nat Neurosci.* 2024 Mar;27(3):449-461. doi: 10.1038/s41593-023-01537-8. Epub 2024 Jan 4. PMID: 38177340; PMCID: PMC10960525.
- Hasan AR, Tasnim F, Aktaruzzaman M, Islam MT, Rayhan R, Brishti A, Hur J, Porter JE, Raihan MO. The Alteration of Microglial Calcium Homeostasis in Central Nervous System Disorders: A Comprehensive Review. *Neuroglia.* 2024; 5(4):410-444. <https://doi.org/10.3390/neuroglia5040027>
- Hayashi T. Sigma-1 receptor: the novel intracellular target of neuropsychotherapeutic drugs. *J Pharmacol Sci.* 2015 Jan;127(1):2-5. doi: 10.1016/j.jphs.2014.07.001. Epub 2014 Dec 9. PMID: 25704011.
- He GL, Liu Y, Li M, Chen CH, Gao P, Yu ZP, Yang XS. The amelioration of phagocytic ability in microglial cells by curcumin through the inhibition of EMF-induced pro-inflammatory responses. *J Neuroinflammation.* 2014 Mar 19;11:49. doi: 10.1186/1742-2094-11-49. PMID: 24645646; PMCID: PMC3994595.
- Heiss K, Vanella L, Murabito P, Prezzavento O, Marrazzo A, Castruccio Castracani C, Barbagallo I, Zappalà A, Arena E, Astuto M, Giarratano A, Li Volti G. (+)-Pentazocine reduces oxidative stress and apoptosis in microglia following hypoxia/reoxygenation injury. *Neurosci Lett.* 2016 Jul 28;626:142-8. doi: 10.1016/j.neulet.2016.05.025. Epub 2016 May 18. Erratum in: *Neurosci Lett.* 2023 Jun 11;807:137247. doi: 10.1016/j.neulet.2023.137247. PMID: 27208832.
- He Y, She H, Zhang T, Xu H, Cheng L, Yepes M, Zhao Y, Mao Z. p38 MAPK inhibits autophagy and promotes microglial inflammatory responses by phosphorylating ULK1. *J Cell Biol.* 2018 Jan 2;217(1):315-328. doi: 10.1083/jcb.201701049. Epub 2017 Dec 1. PMID: 29196462; PMCID: PMC5748971.
- Hines DJ, Hines RM, Mulligan SJ, Macvicar BA. Microglia processes block the spread of damage in the brain and require functional chloride channels. *Glia.* 2009 Nov 15;57(15):1610-8. doi: 10.1002/glia.20874. PMID: 19382211.
- Hoffmann A, Kann O, Ohlemeyer C, Hanisch UK, Kettenmann H. Elevation of basal intracellular calcium as a central element in the activation of brain macrophages (microglia): suppression of receptor-evoked calcium signaling and control of release function. *J Neurosci.* 2003 Jun 1;23(11):4410-9. doi: 10.1523/JNEUROSCI.23-11-04410.2003. PMID: 12805281; PMCID: PMC6740788.

- Hopp SC. Targeting microglia L-type voltage-dependent calcium channels for the treatment of central nervous system disorders. *J Neurosci Res.* 2021 Jan;99(1):141-162. doi: 10.1002/jnr.24585. Epub 2020 Jan 29. PMID: 31997405; PMCID: PMC9394523.
- Ito D, Imai Y, Ohsawa K, Nakajima K, Fukuuchi Y, Kohsaka S. Microglia-specific localisation of a novel calcium binding protein, Iba1. *Brain Res Mol Brain Res.* 1998 Jun 1;57(1):1-9. doi: 10.1016/s0169-328x(98)00040-0. PMID: 9630473.
- Ito D, Tanaka K, Suzuki S, Dembo T, Fukuuchi Y. Enhanced expression of Iba1, ionized calcium-binding adapter molecule 1, after transient focal cerebral ischemia in rat brain. *Stroke.* 2001 May;32(5):1208-15. doi: 10.1161/01.str.32.5.1208. PMID: 11340235.
- Jin LW, Lucente JD, Nguyen HM, Singh V, Singh L, Chavez M, Bushong T, Wulff H, Maezawa I. Repurposing the KCa3.1 inhibitor senicapoc for Alzheimer's disease. *Ann Clin Transl Neurol.* 2019 Mar 18;6(4):723-738. doi: 10.1002/acn3.754. PMID: 31019997; PMCID: PMC6469250.
- Jia J, Cheng J, Wang C, Zhen X. Sigma-1 Receptor-Modulated Neuroinflammation in Neurological Diseases. *Front Cell Neurosci.* 2018 Sep 20;12:314. doi: 10.3389/fncel.2018.00314. PMID: 30294261; PMCID: PMC6158303.
- Jin MM, Wang F, Qi D, Liu WW, Gu C, Mao CJ, Yang YP, Zhao Z, Hu LF, Liu CF. A Critical Role of Autophagy in Regulating Microglia Polarization in Neurodegeneration. *Front Aging Neurosci.* 2018 Nov 20;10:378. doi: 10.3389/fnagi.2018.00378. PMID: 30515090; PMCID: PMC6256089.
- Kata D, Földesi I, Feher LZ, Hackler L Jr, Puskas LG, Gulya K. A novel pleiotropic effect of aspirin: Beneficial regulation of pro- and anti-inflammatory mechanisms in microglial cells. *Brain Res Bull.* 2017 Jun;132:61-74. doi: 10.1016/j.brainresbull.2017.05.009. Epub 2017 May 18. PMID: 28528204.
- Kata D, Földesi I, Feher LZ, Hackler L Jr, Puskas LG, Gulya K. Rosuvastatin enhances anti-inflammatory and inhibits pro-inflammatory functions in cultured microglial cells. *Neuroscience.* 2016 Feb 9;314:47-63. doi: 10.1016/j.neuroscience.2015.11.053. Epub 2015 Nov 26. PMID: 26633263.
- Kazama I, Maruyama Y, Matsubara M. Benidipine persistently inhibits delayed rectifier K(+)-channel currents in murine thymocytes. *Immunopharmacol Immunotoxicol.* 2013 Feb;35(1):28-33. doi: 10.3109/08923973.2012.723011. Epub 2012 Sep 17. PMID: 22978806.

- Kettenmann H, Hoppe D, Gottmann K, Banati R, Kreutzberg G. Cultured microglial cells have a distinct pattern of membrane channels different from peritoneal macrophages. *J Neurosci Res.* 1990 Jul;26(3):278-87. doi: 10.1002/jnr.490260303. PMID: 1697905.
- Kettenmann H, Hanisch UK, Noda M, Verkhratsky A. Physiology of microglia. *Physiol Rev.* 2011 Apr;91(2):461-553. doi: 10.1152/physrev.00011.2010. PMID: 21527731.
- Kigerl KA, de Rivero Vaccari JP, Dietrich WD, Popovich PG, Keane RW. Pattern recognition receptors and central nervous system repair. *Exp Neurol.* 2014 Aug;258:5-16. doi: 10.1016/j.expneurol.2014.01.001. PMID: 25017883; PMCID: PMC4974939.
- Klionsky DJ. Autophagy: from phenomenology to molecular understanding in less than a decade. *Nat Rev Mol Cell Biol.* 2007 Nov;8(11):931-7. doi: 10.1038/nrm2245. PMID: 17712358.
- Kreutzberg GW. Microglia: a sensor for pathological events in the CNS. *Trends Neurosci.* 1996 Aug;19(8):312-8. doi: 10.1016/0166-2236(96)10049-7. PMID: 8843599.
- Lam D, Lively S, Schlichter LC. Responses of rat and mouse primary microglia to pro- and anti-inflammatory stimuli: molecular profiles, K⁺ channels and migration. *J Neuroinflammation.* 2017 Aug 22;14(1):166. doi: 10.1186/s12974-017-0941-3. PMID: 28830445; PMCID: PMC5567442.
- Laskowitz DT, Kolls BJ. Neuroprotection in subarachnoid hemorrhage. *Stroke.* 2010 Oct;41(10 Suppl):S79-84. doi: 10.1161/STROKEAHA.110.595090. PMID: 20876512; PMCID: PMC3376008.
- Leal-Lasarte MM, Franco JM, Labrador-Garrido A, Pozo D, Roodveldt C. Extracellular TDP-43 aggregates target MAPK/MAK/MRK overlapping kinase (MOK) and trigger caspase-3/IL-18 signaling in microglia. *FASEB J.* 2017 Jul;31(7):2797-2816. doi: 10.1096/fj.201601163R. Epub 2017 Mar 23. PMID: 28336525.
- Lee JW, Nam H, Kim LE, Jeon Y, Min H, Ha S, Lee Y, Kim SY, Lee SJ, Kim EK, Yu SW. TLR4 (toll-like receptor 4) activation suppresses autophagy through inhibition of FOXO3 and impairs phagocytic capacity of microglia. *Autophagy.* 2019 May;15(5):753-770. doi: 10.1080/15548627.2018.1556946. Epub 2018 Dec 13. PMID: 30523761; PMCID: PMC6526818.
- Leyh J, Paeschke S, Mages B, Michalski D, Nowicki M, Bechmann I, Winter K. Classification of Microglial Morphological Phenotypes Using Machine Learning. *Front Cell Neurosci.* 2021 Jun 29;15:701673. doi: 10.3389/fncel.2021.701673. PMID: 34267628; PMCID: PMC8276040.

- Li Y, Hu X, Liu Y, Bao Y, An L. Nimodipine protects dopaminergic neurons against inflammation-mediated degeneration through inhibition of microglial activation. *Neuropharmacology*. 2009 Mar;56(3):580-9. doi: 10.1016/j.neuropharm.2008.10.016. Epub 2008 Nov 21. PMID: 19049811.
- Lian L, Zhang Y, Liu L, Yang L, Cai Y, Zhang J, Xu S. Neuroinflammation in Ischemic Stroke: Focus on MicroRNA-mediated Polarization of Microglia. *Front Mol Neurosci*. 2021 Jan 7;13:612439. doi: 10.3389/fnmol.2020.612439. PMID: 33488360; PMCID: PMC7817943.
- Lowry OH, Rosebrough NJ, Farr AL, Randall RJ. Protein measurement with the Folin phenol reagent. *J Biol Chem*. 1951 Nov;193(1):265-75. PMID: 14907713.
- Lu X, Chen L, Chen Y, Shao Q, Qin W. Bafilomycin A1 inhibits the growth and metastatic potential of the BEL-7402 liver cancer and HO-8910 ovarian cancer cell lines and induces alterations in their microRNA expression. *Exp Ther Med*. 2015 Nov;10(5):1829-1834. doi: 10.3892/etm.2015.2758. Epub 2015 Sep 22. PMID: 26640557; PMCID: PMC4665926.
- Lue LF, Schmitz C, Walker DG. What happens to microglial TREM2 in Alzheimer's disease: Immunoregulatory turned into immunopathogenic? *Neuroscience*. 2015 Aug 27;302:138-50. doi: 10.1016/j.neuroscience.2014.09.050. Epub 2014 Oct 2. PMID: 25281879.
- Luo L, Song S, Ezenwukwa CC, Jalali S, Sun B, Sun D. Ion channels and transporters in microglial function in physiology and brain diseases. *Neurochem Int*. 2021 Jan;142:104925. doi: 10.1016/j.neuint.2020.104925. Epub 2020 Nov 26. PMID: 33248207; PMCID: PMC7895445.
- Maguire E, Connor-Robson N, Shaw B, O'Donoghue R, Stöberl N, Hall-Roberts H. Assaying Microglia Functions In Vitro. *Cells*. 2022 Oct 28;11(21):3414. doi: 10.3390/cells11213414. PMID: 36359810; PMCID: PMC9654693.
- Mastinu A, Anyanwu M, Carone M, Abate G, Bonini SA, Peron G, Tirelli E, Pucci M, Ribaud G, Oselladore E, Premoli M, Gianoncelli A, Uberti DL, Memo M. The Bright Side of Psychedelics: Latest Advances and Challenges in Neuropharmacology. *Int J Mol Sci*. 2023 Jan 10;24(2):1329. doi: 10.3390/ijms24021329. PMID: 36674849; PMCID: PMC9865175.
- Meneses G, Bautista M, Florentino A, Díaz G, Acero G, Besedovsky H, Meneses D, Fleury A, Del Rey A, Gevorkian G, Fragoso G, Scitutto E. Electric stimulation of the vagus nerve reduced mouse neuroinflammation induced by lipopolysaccharide. *J Inflamm (Lond)*.

- 2016 Oct 29;13:33. doi: 10.1186/s12950-016-0140-5. PMID: 27807399; PMCID: PMC5086408.
- Meyer H, Wehinger E, Bossert F, Scherling D. Nimodipine: synthesis and metabolic pathway. *Arzneimittelforschung*. 1983;33(1):106-12. doi: 10.1002/chin.198320206. PMID: 6681961.
- Mironova GY, Haghbin N, Welsh DG. Functional tuning of Vascular L-type Ca²⁺ channels. *Front Physiol*. 2022 Nov 15;13:1058744. doi: 10.3389/fphys.2022.1058744. PMID: 36457306; PMCID: PMC9705771.
- Montilla A, Zabala A, Matute C, Domercq M. Functional and Metabolic Characterization of Microglia Culture in a Defined Medium. *Front Cell Neurosci*. 2020 Feb 7;14:22. doi: 10.3389/fncel.2020.00022. PMID: 32116565; PMCID: PMC7025516.
- Mori T, Hayashi T, Hayashi E, Su TP. Sigma-1 receptor chaperone at the ER-mitochondrion interface mediates the mitochondrion-ER-nucleus signaling for cellular survival. *PLoS One*. 2013 Oct 18;8(10):e76941. doi: 10.1371/journal.pone.0076941. PMID: 24204710; PMCID: PMC3799859.
- Mugume Y, Kazibwe Z, Bassham DC. Target of rapamycin in control of autophagy: Puppet master and signal integrator. *Int J Mol Sci* (2020) 21(21):8259. doi: 10.3390/ijms21218259.
- Miyake T, Shirakawa H, Kusano A, Sakimoto S, Konno M, Nakagawa T, Mori Y, Kaneko S. TRPM2 contributes to LPS/IFN γ -induced production of nitric oxide via the p38/JNK pathway in microglia. *Biochem Biophys Res Commun*. 2014 Feb 7;444(2):212-7. doi: 10.1016/j.bbrc.2014.01.022.
- Nardai S, László M, Szabó A, Alpár A, Hanics J, Zahola P, Merkely B, Frecska E, Nagy Z. N,N-dimethyltryptamine reduces infarct size and improves functional recovery following transient focal brain ischemia in rats. *Exp Neurol*. 2020 May;327:113245. doi: 10.1016/j.expneurol.2020.113245. Epub 2020 Feb 14. PMID: 32067950.
- Nimmerjahn A, Kirchhoff F, Helmchen F. Resting microglial cells are highly dynamic surveillants of brain parenchyma in vivo. *Science*. 2005 May 27;308(5726):1314-8. doi: 10.1126/science.1110647. Epub 2005 Apr 14. PMID: 15831717.
- Norris GT, Kipnis J. Immune cells and CNS physiology: Microglia and beyond. *J Exp Med*. 2019 Jan 7;216(1):60-70. doi: 10.1084/jem.20180199. Epub 2018 Nov 30. PMID: 30504438; PMCID: PMC6314530.
- Ooi K, Hu L, Feng Y, Han C, Ren X, Qian X, Huang H, Chen S, Shi Q, Lin H, Wang J, Zhu D, Wang R, Xia C. Sigma-1 Receptor Activation Suppresses Microglia M1 Polarization via

- Regulating Endoplasmic Reticulum-Mitochondria Contact and Mitochondrial Functions in Stress-Induced Hypertension Rats. *Mol Neurobiol.* 2021 Dec;58(12):6625-6646. doi: 10.1007/s12035-021-02488-6. Epub 2021 Oct 2. PMID: 34601668.
- Paresce DM, Ghosh RN, Maxfield FR. Microglial cells internalize aggregates of the Alzheimer's disease amyloid beta-protein via a scavenger receptor. *Neuron.* 1996 Sep;17(3):553-65. doi: 10.1016/s0896-6273(00)80187-7. PMID: 8816718.
- Parzych KR, Klionsky DJ. An overview of autophagy: morphology, mechanism, and regulation. *Antioxid Redox Signal.* 2014 Jan 20;20(3):460-73. doi: 10.1089/ars.2013.5371. Epub 2013 Aug 2. PMID: 23725295; PMCID: PMC3894687.
- Pedemonte N, Diena T, Caci E, Nieddu E, Mazzei M, Ravazzolo R, Zegarra-Moran O, Galietta LJ. Antihypertensive 1,4-dihydropyridines as correctors of the cystic fibrosis transmembrane conductance regulator channel gating defect caused by cystic fibrosis mutations. *Mol Pharmacol.* 2005 Dec;68(6):1736-46. doi: 10.1124/mol.105.015149. Epub 2005 Sep 8. PMID: 16150931.
- Peng L, Hu G, Yao Q, Wu J, He Z, Law BY, Hu G, Zhou X, Du J, Wu A, Yu L. Microglia autophagy in ischemic stroke: A double-edged sword. *Front Immunol.* 2022 Nov 16;13:1013311. doi: 10.3389/fimmu.2022.1013311. PMID: 36466850; PMCID: PMC9708732.
- Penke B, Fulop L, Szucs M, Frecska E. The Role of Sigma-1 Receptor, an Intracellular Chaperone in Neurodegenerative Diseases. *Curr Neuropharmacol.* 2018;16(1):97-116. doi: 10.2174/1570159X15666170529104323. PMID: 28554311; PMCID: PMC5771390.
- Perry VH, Teeling J. Microglia and macrophages of the central nervous system: the contribution of microglia priming and systemic inflammation to chronic neurodegeneration. *Semin Immunopathol.* 2013 Sep;35(5):601-12. doi: 10.1007/s00281-013-0382-8. Epub 2013 Jun 4. PMID: 23732506; PMCID: PMC3742955.
- Pesti I, Barczánfalvi G, Dulka K, Kata D, Farkas E, Gulya K. Bafilomycin 1A Affects p62/SQSTM1 Autophagy Marker Protein Level and Autophagosome Puncta Formation Oppositely under Various Inflammatory Conditions in Cultured Rat Microglial Cells. *Int J Mol Sci.* 2024 Jul 29;25(15):8265. doi: 10.3390/ijms25158265. PMID: 39125836; PMCID: PMC11311604.
- Pesti I, Légrádi Á, Farkas E. Primary microglia cell cultures in translational research: Strengths and limitations. *J Biotechnol.* 2024 May 10;386:10-18. doi: 10.1016/j.jbiotec.2024.03.005. Epub 2024 Mar 20. PMID: 38519034.

- Qin C, Liu Q, Hu ZW, Zhou LQ, Shang K, Bosco DB, Wu LJ, Tian DS, Wang W. Microglial TLR4-dependent autophagy induces ischemic white matter damage via STAT1/6 pathway. *Theranostics*. 2018 Oct 29;8(19):5434-5451. doi: 10.7150/thno.27882. Erratum in: *Theranostics*. 2020 Jul 10;10(19):8818-8820. doi: 10.7150/thno.49958. PMID: 30555556; PMCID: PMC6276098.
- Qin J, Ma Z, Chen X, Shu S. Microglia activation in central nervous system disorders: A review of recent mechanistic investigations and development efforts. *Front Neurol*. 2023 Mar 7;14:1103416. doi: 10.3389/fneur.2023.1103416. PMID: 36959826; PMCID: PMC10027711.
- Raghunatha P, Vosoughi A, Kauppinen TM, Jackson MF. Microglial NMDA receptors drive pro-inflammatory responses via PARP-1/TRMP2 signaling. *Glia*. 2020 Jul;68(7):1421-1434. doi: 10.1002/glia.23790.
- Ren P, Wang J, Li N, Li G, Ma H, Zhao Y, Li Y. Sigma-1 Receptors in Depression: Mechanism and Therapeutic Development. *Front Pharmacol*. 2022 Jun 16;13:925879. doi: 10.3389/fphar.2022.925879. PMID: 35784746; PMCID: PMC9243434.
- Roqué PJ, Costa LG. Co-Culture of Neurons and Microglia. *Curr Protoc Toxicol*. 2017 Nov 8;74:11.24.1-11.24.17. doi: 10.1002/cptx.32. PMID: 29117434; PMCID: PMC5774987.
- Rumianek AN, Greaves DR. How Have Leukocyte In Vitro Chemotaxis Assays Shaped Our Ideas about Macrophage Migration? *Biology (Basel)*. 2020 Dec 2;9(12):439. doi: 10.3390/biology9120439. PMID: 33276594; PMCID: PMC7761587.
- Ruscher K, Inácio AR, Valind K, Rowshan Ravan A, Kuric E, Wieloch T. Effects of the sigma-1 receptor agonist 1-(3,4-dimethoxyphenethyl)-4-(3-phenylpropyl)-piperazine dihydrochloride on inflammation after stroke. *PLoS One*. 2012;7(9):e45118. doi: 10.1371/journal.pone.0045118. Epub 2012 Sep 18. PMID: 23028794; PMCID: PMC3445585.
- Saddala MS, Lennikov A, Mukwaya A, Yang Y, Hill MA, Lagali N, Huang H. Discovery of novel L-type voltage-gated calcium channel blockers and application for the prevention of inflammation and angiogenesis. *J Neuroinflammation*. 2020 Apr 25;17(1):132. doi: 10.1186/s12974-020-01801-9. PMID: 32334630; PMCID: PMC7183139.
- Santiago JV, Natu A, Ramelow CC, Rayaprolu S, Xiao H, Kumar V, Kumar P, Seyfried NT, Rangaraju S. Identification of State-Specific Proteomic and Transcriptomic Signatures of Microglia-Derived Extracellular Vesicles. *Mol Cell Proteomics*. 2023 Dec;22(12):100678. doi: 10.1016/j.mcpro.2023.100678. Epub 2023 Nov 11. PMID: 37952696; PMCID: PMC10755493.

- Scriabine A, van den Kerckhoff W. Pharmacology of nimodipine. A review. *Ann N Y Acad Sci.* 1988;522:698-706. doi: 10.1111/j.1749-6632.1988.tb33415.x. PMID: 3288065.
- Sebastian-Valverde M, Wu H, Al Rahim M, Sanchez R, Kumar K, De Vita RJ, Pasinetti GM. Discovery and characterization of small-molecule inhibitors of NLRP3 and NLRC4 inflammasomes. *J Biol Chem.* 2021 Jan-Jun;296:100597. doi: 10.1016/j.jbc.2021.100597. Epub 2021 Mar 26. PMID: 33781745; PMCID: PMC8095128.
- Sharma P, Ping L. Calcium ion influx in microglial cells: physiological and therapeutic significance. *J Neurosci Res.* 2014 Apr;92(4):409-23. doi: 10.1002/jnr.23344. Epub 2014 Jan 24. PMID: 24464907.
- Shi FJ, Xie H, Zhang CY, Qin HF, Zeng XW, Lou H, Zhang L, Xu GT, Zhang JF, Xu GX. Is Iba-1 protein expression a sensitive marker for microglia activation in experimental diabetic retinopathy? *Int J Ophthalmol.* 2021 Feb 18;14(2):200-208. doi: 10.18240/ijo.2021.02.04. PMID: 33614447; PMCID: PMC7840370.
- Shi J, Johansson J, Woodling NS, Wang Q, Montine TJ, Andreasson K. The prostaglandin E2 E-prostanoid 4 receptor exerts anti-inflammatory effects in brain innate immunity. *J Immunol.* 2010 Jun 15;184(12):7207-18. doi: 10.4049/jimmunol.0903487. Epub 2010 May 7. PMID: 20483760; PMCID: PMC3103215.
- Shi Y, Yamada K, Liddel SA, Smith ST, Zhao L, Luo W, Tsai RM, Spina S, Grinberg LT, Rojas JC, Gallardo G, Wang K, Roh J, Robinson G, Finn MB, Jiang H, Sullivan PM, Baufeld C, Wood MW, Sutphen C, McCue L, Xiong C, Del-Aguila JL, Morris JC, Cruchaga C; Alzheimer's Disease Neuroimaging Initiative; Fagan AM, Miller BL, Boxer AL, Seeley WW, Butovsky O, Barres BA, Paul SM, Holtzman DM. ApoE4 markedly exacerbates tau-mediated neurodegeneration in a mouse model of tauopathy. *Nature.* 2017 Sep 28;549(7673):523-527. doi: 10.1038/nature24016. Epub 2017 Sep 20. PMID: 28959956; PMCID: PMC5641217.
- Sierra A, Abiega O, Shahraz A, Neumann H. Janus-faced microglia: beneficial and detrimental consequences of microglial phagocytosis. *Front Cell Neurosci.* 2013 Jan 30;7:6. doi: 10.3389/fncel.2013.00006. PMID: 23386811; PMCID: PMC3558702.
- Sin JH, Shafeeq H, Levy ZD. Nimodipine for the treatment of otolaryngic indications. *Am J Health Syst Pharm.* 2018 Sep 15;75(18):1369-1377. doi: 10.2146/ajhp170677. PMID: 30190294.
- Smith AM, Dragunow M. The human side of microglia. *Trends Neurosci.* 2014 Mar;37(3):125-35. doi: 10.1016/j.tins.2013.12.001. Epub 2014 Jan 2. PMID: 24388427.

- Smith RL, Canton H, Barrett RJ, Sanders-Bush E. Agonist properties of N,N-dimethyltryptamine at serotonin 5-HT_{2A} and 5-HT_{2C} receptors. *Pharmacol Biochem Behav.* 1998 Nov;61(3):323-30. doi: 10.1016/s0091-3057(98)00110-5. PMID: 9768567.
- Szabo A, Kovacs A, Riba J, Djurovic S, Rajnavolgyi E, Frecska E. The Endogenous Hallucinogen and Trace Amine N,N-Dimethyltryptamine (DMT) Displays Potent Protective Effects against Hypoxia via Sigma-1 Receptor Activation in Human Primary iPSC-Derived Cortical Neurons and Microglia-Like Immune Cells. *Front Neurosci.* 2016 Sep 14;10:423. doi: 10.3389/fnins.2016.00423. PMID: 27683542; PMCID: PMC5021697.
- Szabó Í, Varga VÉ, Dvorácskó S, Farkas AE, Körmöczi T, Berkecz R, Kecskés S, Menyhárt Á, Frank R, Hantosi D, Cozzi NV, Frecska E, Tömböly C, Krizbai IA, Bari F, Farkas E. N,N-Dimethyltryptamine attenuates spreading depolarization and restrains neurodegeneration by sigma-1 receptor activation in the ischemic rat brain. *Neuropharmacology.* 2021 Jul 1;192:108612. doi: 10.1016/j.neuropharm.2021.108612. Epub 2021 May 21. PMID: 34023338.
- Szabo M, Gulya K. Development of the microglial phenotype in culture. *Neuroscience.* 2013 Jun 25;241:280-95. doi: 10.1016/j.neuroscience.2013.03.033.
- Timmerman R, Burm SM, Bajramovic JJ. An Overview of *in vitro* Methods to Study Microglia. *Front Cell Neurosci.* 2018 Aug 6;12:242. doi: 10.3389/fncel.2018.00242. PMID: 30127723; PMCID: PMC6087748.
- Tremblay MÈ, Stevens B, Sierra A, Wake H, Bessis A, Nimmerjahn A. The role of microglia in the healthy brain. *J Neurosci.* 2011 Nov 9;31(45):16064-9. doi: 10.1523/JNEUROSCI.4158-11.2011. PMID: 22072657; PMCID: PMC6633221.
- Wang H, Li J, Zhang H, Wang M, Xiao L, Wang Y, Cheng Q. Regulation of microglia polarization after cerebral ischemia. *Front Cell Neurosci.* 2023 Jun 8;17:1182621. doi: 10.3389/fncel.2023.1182621. PMID: 37361996; PMCID: PMC10285223.
- Wang S, Zhang J, Zhang J, Li A, Yuan Z, Cheng J. (2024). Roles of microglial calcium channels in neurodegenerative diseases. *Human Brain.* 3. 10.37819/hb.1.1806.
- Wang Y, Tian J, Liu D, Li T, Mao Y, Zhu C. Microglia in radiation-induced brain injury: Cellular and molecular mechanisms and therapeutic potential. *CNS Neurosci Ther.* 2024 Jun;30(6):e14794. doi: 10.1111/cns.14794. PMID: 38867379; PMCID: PMC11168970.
- Warden AS, Han C, Hansen E, Trescott S, Nguyen C, Kim R, Schafer D, Johnson A, Wright M, Ramirez G, Lopez-Sanchez M, Coufal NG. Tools for studying human microglia: In vitro

- and in vivo strategies. *Brain Behav Immun.* 2023 Jan;107:369-382. doi: 10.1016/j.bbi.2022.10.008. Epub 2022 Nov 3. PMID: 36336207; PMCID: PMC9810377.
- Wendimu MY, Hooks SB. Microglia Phenotypes in Aging and Neurodegenerative Diseases. *Cells.* 2022 Jun 30;11(13):2091. doi: 10.3390/cells11132091. PMID: 35805174; PMCID: PMC9266143.
- Weng TY, Tsai SA, Su TP. Roles of sigma-1 receptors on mitochondrial functions relevant to neurodegenerative diseases. *J Biomed Sci.* 2017 Sep 16;24(1):74. doi: 10.1186/s12929-017-0380-6. PMID: 28917260; PMCID: PMC5603014.
- Wiens KR, Brooks NAH, Riar I, Greuel BK, Lindhout IA, Klegeris A. Psilocin, the Psychoactive Metabolite of Psilocybin, Modulates Select Neuroimmune Functions of Microglial Cells in a 5-HT₂ Receptor-Dependent Manner. *Molecules.* 2024 Oct 28;29(21):5084. doi: 10.3390/molecules29215084. PMID: 39519725; PMCID: PMC11547910.
- Witting A, Möller T. Microglia cell culture: a primer for the novice. *Methods Mol Biol.* 2011;758:49-66. doi: 10.1007/978-1-61779-170-3_4. PMID: 21815058.
- Xie Z, Xie Y, Xu Y, Zhou H, Xu W, Dong Q. Bafilomycin A1 inhibits autophagy and induces apoptosis in MG63 osteosarcoma cells. *Mol Med Rep.* 2014 Aug;10(2):1103-7. doi: 10.3892/mmr.2014.2281. Epub 2014 May 29. PMID: 24890793.
- Xiong XY, Liu L, Yang QW. Functions and mechanisms of microglia/macrophages in neuroinflammation and neurogenesis after stroke. *Prog Neurobiol.* 2016 Jul;142:23-44. doi: 10.1016/j.pneurobio.2016.05.001. Epub 2016 May 7. PMID: 27166859.
- Yang CS, Yuk JM, Shin DM, Kang J, Lee SJ, Jo EK. Secretory phospholipase A2 plays an essential role in microglial inflammatory responses to *Mycobacterium tuberculosis*. *Glia.* 2009 Aug 1;57(10):1091-103. doi: 10.1002/glia.20832. PMID: 19115385.
- Ye X, Zhu M, Che X, Wang H, Liang XJ, Wu C, Xue X, Yang J. Lipopolysaccharide induces neuroinflammation in microglia by activating the MTOR pathway and downregulating Vps34 to inhibit autophagosome formation. *J Neuroinflammation.* 2020 Jan 11;17(1):18. doi: 10.1186/s12974-019-1644-8. PMID: 31926553; PMCID: PMC6954631.
- Zhang G, Li Q, Tao W, Qin P, Chen J, Yang H, Chen J, Liu H, Dai Q, Zhen X. Sigma-1 receptor-regulated efferocytosis by infiltrating circulating macrophages/microglial cells protects against neuronal impairments and promotes functional recovery in cerebral ischemic stroke. *Theranostics.* 2023 Jan 1;13(2):543-559. doi: 10.7150/thno.77088. PMID: 36632219; PMCID: PMC9830433.

Zhang Y, Feng S, Nie K, Li Y, Gao Y, Gan R, Wang L, Li B, Sun X, Wang L, Zhang Y. TREM2 modulates microglia phenotypes in the neuroinflammation of Parkinson's disease. *Biochem Biophys Res Commun.* 2018 May 23;499(4):797-802. doi: 10.1016/j.bbrc.2018.03.226. Epub 2018 Apr 4. PMID: 29621548.